UNIVERSITY OF SPLIT
SCHOOL OF MEDICINE

DIRK MAYER, MD

EFFECTS OF NEWLY DESIGNED ALBUMIN-DERIVED PERFLUOROCARBON-BASED NANOPARTICLES IN THE THERAPY OF DECOMPRESSION INDUCED GAS EMBOLISMS IN RATS

DISSERTATION

Split, 2023

UNIVERSITY OF SPLIT
SCHOOL OF MEDICINE

DIRK MAYER, MD

EFFECTS OF NEWLY DESIGNED ALBUMIN-DERIVED PERFLUOROCARBON-BASED NANOPARTICLES IN THE THERAPY OF DECOMPRESSION INDUCED GAS EMBOLISMS IN RATS

DISSERTATION

Mentor:

Prof. Katja Bettina Ferenz

Split, 2023

INSTITUTIONS & MENTORS

The studies included in this thesis have been carried out as a cooperation project of the following institutions: University Duisburg-Essen, Institute of Physiology, Institute of Physical Chemistry and Institute of Physiological Chemistry, CENIDE, D-45147 / D-45141 Essen, Germany; Université de Bretagne Occidentale, EA 4324-ORPHY, IBSAM, F-29200 Brest, France; Medical School University of Split, Department of Integrative Physiology, HR-21000 Split, Croatia and REGIOMED Klinikum Coburg, Department of Pathology, D-96450 Coburg, Germany.

The studies were performed during the years 2017-2020 under supervision of my mentors *Prof. Katja Bettina Ferenz* and *Prof. Johannes Brachmann.* An extension study has started in December 2020 and is ongoing.

The present work was performed in fulfilment of the requirements for obtaining the PhD degree within the Clinical Evidence-Based Medicine postgraduate program at USSM.

ACKNOWLEDGEMENTS

Foremost, I would like to express my sincere gratitude to my advisor *Prof. Katja Bettina Ferenz*, University of Duisburg-Essen, for the continuous support of my PhD study and research, for her motivation, patience, and immense knowledge. Her guidance helped me in all the time of research and writing of this thesis.

I would like to thank *Prof. François Guerrero* and *Prof. Christelle Goanvec*, Université de Bretagne Occidentale, *Prof. Johannes Brachmann*, Department of Cardiology, Coburg and *Prof. Christian Mayer*, University of Duisburg-Essen for their great support and encouragement, insightful comments, and fruitful discussions on this manuscript.

My sincere thanks also goes to *Prof. Marko Ljubkovic* and *Prof. Jasna Marinović*, University of Split, for giving the decisive impetus for this work. Without their constant help this project would not have been possible.

The excellent technical assistance of *Ms. Eva Hillen, Ms. Annika Stokvis, Ms. Alexandra Scheer, Mr. Johannes Jaegers,* and *Mr. Falk Kaehler* is gratefully acknowledged. I thank *Mr. Robert Mayer* for help in creating the graphics and *Dr. Patrick Biggar* for linguistic and critical revision of the manuscript.

I also wish to express my deep appreciation to *Prof. Ana Jeroncic* and *Dr. Holger Göbel* for improving the statistical analysis and *Dr. Alfons Kreczy* and his team for the excellent histological analysis.

Special thanks to *Ms. Julija Pusic* and *Prof. Ivana Kolčić*, Office for Science, Postgraduate Studies and Continuing Medical Education, University of Split, for their strong support during the whole PhD process.

Last, but not least, my warm and heartfelt thanks go to my family.

TABLE OF CONTENTS

1. INTRODUCTION 1
1.1. Decompression sickness: Aspects of Pathophysiology 1
1.2. Conventional treatment of DCS 4
1.3. Critical assessment of a rat model for the investigation of DCS 4
1.4. Perfluorocarbons: Physiochemical properties 6
1.5. Perfluorocarbons for intravenous use 9
1.6. Perfluorocarbon-based preparations in the treatment of DCS 10
1.6.1. Preclinical studies 11
1.6.2. Perfluorocarbon-based preparations in clinical trials 13
1.7. Albumin-derived artificial oxygen carriers as a new concept 16
2. AIM OF THE STUDY 19
3. METHODS 20
3.1. Materials 20
3.2. Synthesis of nanocapsules 20
3.3. Determination of size of nanocapsules 21
3.4. Animal experiments 21
3.5. Test groups 24
3.6. Hyperbaric protocol 24
3.7. Clinical observation following decompression 26
3.8. Blood sampling 26
3.9. Determination of plasma parameters 27
3.10. Tissue sampling 27
3.11. Histological evaluation of organs 28
3.12. Statistical analysis 28
4. RESULTS 29
4.1. Occurrence and severity of DCS 29
4.2. Survival in DCS 30
4.3. Results of autopsy 32
4.4. Histological assessment 33
4.4.1. Liver 33
4.4.2. Kidney 40
4.4.3. Spleen 42
4.5. Plasma parameters 45

5. DISCUSSION 47
6. CONCLUSIONS 53
7. SUMMARY 54
8. SAŽETAK 55
9. CURRICULUM VITAE 57
10. REFERENCES 60

ABBREVIATIONS

A-AOCs..... albumin-derived perfluorocarbon-based artificial oxygen carriers
AGE..... arterial gas embolism
ALT ..... alanine aminotransferase
A-O-N..... albumin-derived neutral oil-based nanocapsules
AST .....aspartate aminotransferase
CARPA..... complement activation pseudoallergy
CK ..... creatine kinase
CO_2 ..... carbon dioxide
DCI ..... decompression illness
DCS ..... decompression sickness
DDFPe..... dodecafluoropentane
kPa..... kilopascals
LDH..... lactate dehydrogenase
N_2..... nitrogen
NAD/NADP ..... nicotinamide adenine dinucleotide / phosphate
O_2..... oxygen
P ..... pressure
P-Amylase .....pancreatic amylase
PAP..... pulmonary arterial pressure
PFC..... perfluorocarbons
PFD..... perfluorodecalin
VGE..... venous gas emboli

TABLES

Table 1. PFC-preparations and main reasons for rejection by official authorities. 11
Table 2: Description of DCS symptoms. 29
Table 3. Post-experimental plasma parameters. 46

FIGURES

Figure 1. Decompression illness: Overview of clinical forms, pathophysiology, symptoms, treatment 3
Figure 2. Carbon-fluorine-bond 7
Figure 3. Structure of Perfluorodecalin. 7
Figure 4. Comparison of the O_2 capacity of water and PFC at the same pO_2 8
Figure 5. Albumin-derived perfluorocarbon-based artificial oxygen carrier 10
Figure 6. Interaction of PFCs with tissue and blood 16
Figure 7. Pickering effect 17
Figure 8. Transport of nitrogen to the lungs by PFD-nanocapsules 18
Figure 9. Time chart of the experimental set-up 22
Figure 10. Injection of the test substance via the tail vein 23
Figure 11. Two glass containers on left show precipitation of nanocapsules 23
Figure 12. Opened 130-l steel decompression chamber 25
Figure 13. Time chart of the simulated diving profile 25
Figure 14. Occurrence of 3 levels of DCS 30
Figure 15. Survival time 31
Figure 16. Survival probability 32
Figure 17. Foamy blood in the portal and mesenteric veins (animal of the control group) 33
Figure 18 A. Liver, vacuolisation score 34
Figure 18 B. Example for histology of the liver, vacuolisation grade 0 35
Figure 18 C. Example for histology of the liver, vacuolisation grade 3 35
Figure 19 A. Liver, circulatory disorder score 36
Figure 19 B. Histology of the liver, circulatory disorder grade 0 37
Figure 19 C. Histology of the liver, circulatory disorder grade 3 37
Figure 20. Liver, hepatocyte damage score 38
Figure 21 A. Liver, sinusoid congestion score 38
Figure 21 B. Histology of the liver, sinusoid congestion grade 0 39
Figure 21 C. Histology of the liver, sinusoid congestion grade 3 39
Figure 22 A. Kidney, blood in the medullo-cortical junction score 40
Figure 22 B. Histology kidney, blood accumulation medullo-cortical junction grade 0 41
Figure 22 C. Histology kidney, blood accumulation medullo-cortical junction grade 3 41
Figure 23 A. Spleen, accumulation of macrophages score 42

Figure 23 B. Histology, macrophages in the spleen grade 0 43
Figure 23 C. Histology, macrophages in the spleen grade 3 43
Figure 24 A. Spleen, accumulation of blood score 44
Figure 24 B. Histology of the spleen, accumulation of blood grade 0 44
Figure 24 C. Histology of the spleen, accumulation of blood grade 3 45

INTRODUCTION

1.1. Decompression sickness: Aspects of Pathophysiology

Decompression sickness (DCS) is a systemic pathophysiological process characterized by a broad spectrum of symptoms, occurring among people exposed to pressure differentials (e.g., scuba divers, airplane pilots, hyperbaric chamber workers, or astronauts). Symptoms range from skin rash to severe neurological impairment such as paralysis, and DCS may even result in death (1). Sudden decrease of ambient pressure, for example, in the case of a diver ascending too quickly or a rapid drop in cabin pressure in an airplane, leads to increase in size of extra- and intravascular bubbles when the sum of the dissolved gas tensions (oxygen, carbon dioxide, nitrogen, helium) and water vapor exceeds the local absolute pressure (1-3). The evolution of these bubbles in vivo is a subject of research and controversial discussions. It can be assumed that de novo bubble formation is not relevant because a pressure gradient ($P_{tissue}N_2/P_{ambient\ pressure}$) of several atmospheres would be necessary for this process (4). Alternatively, hydrophobic spots are a possible starting point with pre-existing micro bubbles adherent to the endothelium, or phospholipid spots localized on the lumen-vessel wall (5-8). *Thom et al.* demonstrated that nitrogen dioxide is a nascent gas nucleation site synthesized in some microparticles and possibly responsible for initiating postdecompression inflammatory injuries (9).

Intravascular gas bubbles are coated with proteins which interact with the surroundings (10). In the further course, arising venous gas emboli are associated with different effects on blood vessels, including inflammation, clotting and complement activation (11) as central mechanisms of DCS. However, there are also critics of this pathophysiological theory: *Madden et al.* hypothesized that gas bubbles are rather an exacerbating factor in DCS. They postulated that endothelial dysfunction caused by a temporary loss of homeostasis due to increased total oxidant status could be the main cause (12).

Sometimes the term decompression illness (DCI) is used to describe the different manifestations. Beside the described venous gas emboli (VGE), pulmonary barotrauma can be the triggering factor for arterial gas embolism (AGE). Gas bubbles in the arterial system can lead to vascular obstruction, endothelial lesions, ischemia, and inflammation. According to a study by *Wang et al.*(13), reactive oxygen species (also called oxygen free radicals) and bubbles generated during diving and/or decompression led to embolic or biochemical stress and DCS.

Obad et al. could demonstrate that long-term antioxidant treatment reduces the endothelial dysfunction in divers (14). AGE can apparently also result from venous bubbles passing through a patent foramen ovale or other right to left shunt (15), although, this stands in contrast to the results of a recent study that found no correlation between patent foramen ovale, the number of detectable brain white matter lesions on magnetic resonance imaging ("Unidentified Bright Objects") and the results of neuro-psychometric tests (16). **Figure 1** provides an overview of the main pathophysiological mechanisms of DCI and its manifestations as DCS and AGE [modified from (17)].

DCS causes a wide range of symptoms varying from mild complaints (type I, *"the bends"*: musculoskeletal pain) to dangerous consequences including impairment in lung function (*"the chokes"*), cardiovascular failure and serious disorders of the central nervous system associated with lesions in the white matter of the spinal cord (type II) (1,18). In addition to the direct mechanical effects of expanding bubbles, impaired oxygen transport and inflammation lead to further indirect cell injury. Of great importance are negative impacts on the vascular endothelium (19) causing disturbances of platelet aggregation, impairment of tissue repair mechanisms, dysregulation of vascular tone and homeostasis (20). These impacts appear to be dependent on the type of vessel since *Mazur et al.* did not find endothelial dysfunction in aortas from rats suffering DCS (21).

Since decompression-induced vascular bubbles can be quantitatively determined by Doppler ultrasound monitoring and visual two-dimensional ultrasound imaging, these techniques can be used to determine the extent of decompression stress and to improve decompression safety (22,23). *Ljubkovic et al.* described the link between detection of VGE by ultrasound and DCS (24). However, there is no strict correlation between the extent of VGE and the severity of symptoms (11) or endothelial dysfunction (25). Asymptomatic VGE are a very frequent phenomenon that can be observed in up to 50% of divers after decompression from a steady state pressure exposure at an immersion depth of only 3.4 m seawater (2). Concerning the degree of VGE, inter-personal variability plays an important role (26). Furthermore, in contrast to VGE, far less is known about bubble formation in fatty tissue, because detection and quantitative determination in such tissue is much more difficult (27), also, explaining why there is a paucity in reports on the therapeutic effects on extravascular bubbles.

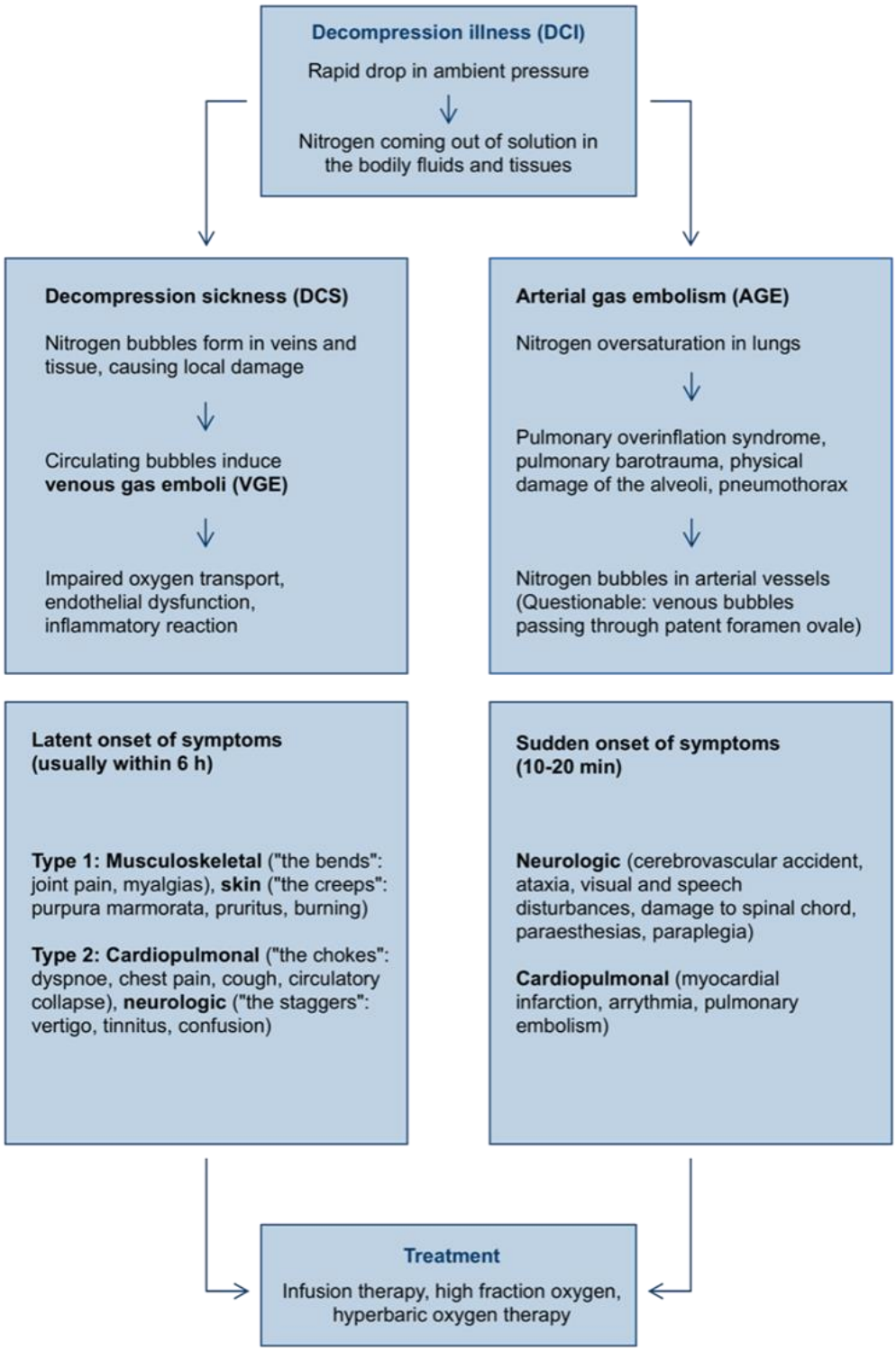

Figure 1. Decompression illness: Overview of clinical forms, pathophysiology, symptoms, treatment.

1.2. **Conventional treatment of DCS**

The standard management for DCS patients is the combination of hyperbaric oxygen-breathing with recompression followed by successive controlled decompression in a hyperbaric chamber (15). The *United States Navy Treatment Table 6* contains a protocol that has proved most effective for severe cases: Maximal pressure of 284 kPa combined with a 100% oxygen atmosphere over 4 hours and 45 minutes, then stepwise decompression (28). This therapy leads to significant nitrogen elimination and improvement of tissue oxygenation enabling reducing the size and number of gas bubbles (29). The success rate for this decompression therapy varies from 50 to 98% (30). But there are disadvantages to this procedure. Substantial human and material resources are necessary. The expensive equipment is frequently not available or only accessible with difficulties, as, for example, transport of the patients expends valuable time. Especially in situations, such as a distressed submarine or an airplane accident with many simultaneously injured persons, the practical feasibility of recompression therapy is limited. Alternative, additional or bridging treatment methods are required (31).

The principles and issues of pre-hospital management of DCS are addressed in a current consensus guideline by *Mitchell et al.(32)*.

1.3. **Critical assessment of a rat model for the investigation of DCS**

Without a doubt it would be unethical to provoke severe DCS in humans for studying purposes. Due to the lack of reliable inanimate physiological models only animals can serve as research objects despite all associated limitations. Several studies have demonstrated a similar kinetic of DCS between humans and large animals such as sheep, goats, or pigs (33,34), but it is obvious that experiments with large mammals are extremely expensive and require high levels of maintenance. Though a rat model is only suitable for the investigation of DCS effects in humans to a limited degree, it has become established for many reasons.

Rattus norvegicus is a convenient research subject, widely available, relatively inexpensive, easily handled, and with a range of physiological characteristics that are similar to those found in humans (35). The majority of rat DCS research has used binary outcomes in the analysis with the classification as dead or alive (36) or DCS versus no DCS (37,38). In some studies survival time was considered (39,40). The diagnosis of DCS in rats is often based upon typical symptoms such as walking difficulties (36-38,41), paralysis (36-38,41), rolling in a rotating cage (37,38,41), convulsions (37,38,42), and respiratory distress (36,37,41,42). Spinal

or neurological signs of DCS are classified in a few studies (43, 44). *Butler et al.* used a score to describe the severity of the observed symptoms (45). Many different objective criteria have been measured to compare the severity of DCS: walking assessment in a rotating cylindrical cage (37,42,46), bubble grades (44,47), platelet counts (44), nitric oxide (45), inflammatory mediators (thromboxane B2 and leukotriene E4) (45) and more.

Arieli et al. (46) could demonstrate that the resistance of rats to DCS is dependent on their weight. Using a hyperbaric protocol with an ambient pressure of 1,110 kPa during 30 min and a decompression rate of 100 kPa/min those animals weighing up to 200 g showed high resistance to DCS. Sensitivity increased linearly between a weight of 250 and 350 g with a 50% DCS death rate. Weight-related sensitivity was explained by increased fat content, enabling the storage of more inert gas, and by a reduction in the specific metabolic rate and tissue perfusion, leading to slower gas clearing, in heavy rats.

There are only a few descriptions of the time course of DCS in the rat. *Spiess et al.* (48) exposed rats to 689 kPa air for 30 min and in case of lethal outcome death occurred within minutes of decompression. This is in accordance with the findings of *Arieli and Lillo et al.(38, 46)*, who described nearly all cases of DCS appearing within the first 30 min of observation. In contrast to humans, rats showed no permanent disability.

Obviously, the effects of simulated chamber diving are in many ways not comparable to those of field scuba diving. Real diving of humans is associated with various environmental stresses influencing hemodynamics and cardiovascular function. Diving studies found an immersion-induced increase in preload, cold-induced increase in afterload, reduction of filling of the left heart due to ventilation of high-density gas mixtures, hyperoxia and formation of intravascular nitrogen bubbles. Scuba diving cannot be performed without psychological stress and exercise is considered as a risk factor for DCS (49). Exercise at depth increases nitrogen uptake consequently to increased blood flow, whereas moderate exercise during decompression will increase gas elimination and reduce the number of venous bubbles detected after diving. *Dujic et al.* found an increased pressure in the pulmonary artery and endothelial dysfunction in diving test persons (50). In contrast simulated diving in a dry chamber is not associated with a change of the PAP. Diving in water produces significantly more gas bubble formation than dry diving (23).

Literature reveals that almost every research group has its own modified dive profile for rats. Most groups use a maximal absolute pressure within 600 to 700 kPa for a „bottom time“ around 60 min. The maximal absolute pressure varies from 500 kPa to 1600 kPa and the

„bottom time“ ranges between 4 to 90 min. For example, *Tang et al.* 2020 (51) applied 600 kPa during 60 min, linear decompression at 200 kPa/min, *Zhang et al.* 2019 (52) 709 kPa during 60 min, linear decompression at 203 kPa/min, *Zhang et al.* 2017 (53) 700 kPa during 90 min, linear decompression 200 kPa/min, *Cosnard et al.* 2017 (54) 900 kPa during 45 min, linear decompression at 6000 kPa/min, *Bao et al.* 2015 (55) 1600 kPa during 4 min, linear decompression at 30 kPa/min, *Sheppard et al.* 2015 (56) 700 kPa during 60 min, *Randsoe et al.* 2015 (57) 506 kPa during 60 min, with decompression stops. In this study, we used the same protocol as *de Maistre et al.* 2016 (58). Compression started at a rate of 100 kPa/min to a pressure of 1000 kPa (90 msw) and then remained constant for 45 minutes. Decompressed down to 200 kPa was performed at a rate of 100 kPa/min with a 5-minute stop at 200 kPa, a 5-minute stop at 160 kPa and a 10-minute stop at 130 kPa. Decompression procedure between 200 kPa and surface took place at a rate of 10 kPa/min.

Most protocols are based on linear decompression. The French working group around *Francois Guerrero* has chosen the described “French” protocol because they have due to closer proximity stronger relations with the French team in Toulon allowing easier and faster transfer of knowledge, and also because the protocol resembles more closely „real dives“ with decompression stops, whereas linear decompression is never used during recreational diving.

The French working group compared the „Norwegian“ protocol to the “French” protocol (59). They observed that the “French” protocol led to a supersaturation of the slower compartments (i.e., with a longer period) but a lower supersaturation of faster compartments than the „Norwegian“ protocol. This resulted in a reduction of DCS by an effect size of –1.1 in favor of the „Norwegian“ protocol.

1.4. **Perfluorocarbons: Physiochemical properties**

In 1966, *Leland C. Clark* and *Frank Gollan* published an experiment of fundamental importance for the further clinical application of fluorinated hydrocarbons (perfluorocarbons, PFC). They demonstrated mice equilibrated with 100% O_2 could dive submersed in fluorobutyltetrahydrofuran (*FX- 80*). The animals were able to “breathe” the fluid maintaining respiration for 4 hours. PFCs proved to function as ideal gas transporters with the potential to store O_2 and to release enough of this respiratory gas to keep mammalians alive (60). The following physicochemical properties are the basis for these experiments:

The hydrogen atoms of PFCs are substituted either completely by fluorine atoms or additional other halogens. An important characteristic of PFC is the high carbon-fluorine bond energy (484 kJ mol-1). This bond is extremely polar, nearly ionic: the probability of the presence of the electron is on the fluorine side (**Figure 2,** used by permission (61)).

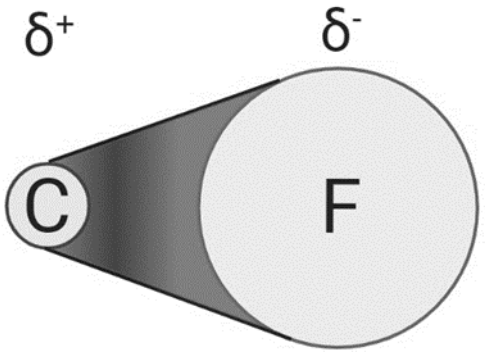

Figure 2. Carbon-fluorine-bond.

However, the molecule as a whole is intrinsically symmetrical annuling the polarity of each C–F bond. As a result, the PFC molecule is nonpolar and insoluble in water. On the other hand, the extreme polarity of the C–F bonds allows no formation of induced dipoles, a precondition for van der Waals forces, necessary for lipid solubility. For these reasons, PFCs belong to the few compounds that are neither hydro- nor lipophile.

What makes PFCs so extraordinary is their extremely high gas-dissolving capacity, depending on the molecular volume of the dissolving gas. It decreases in the order CO_2 >> N_2> O_2 (62). In contrast to the active binding of oxygen to heme, the solubility of respiratory gases in liquid PFC is directly proportional to their partial pressure according to *Henry's law* (63). The two most used PFCs are perfluoroctylbromide (PFOB) and perfluorodecalin (PFD, **Figure 3**, used by permission (61)).

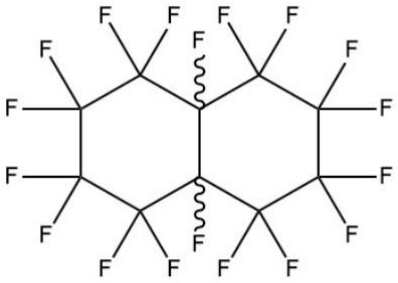

Figure 3. Structure of Perfluorodecalin.

The solubility of O_2 in PFD is 403 mL_{O2} / L_{PFD} at 1 atm (1 bar, 760 mmHg), compared to 6,3 mL_{O2} / L_{H2O} and 200 mL_{O2} / L_{blood}. Carbon dioxide can be dissolved in PFD up to 4 times the amount of O_2 (62). When making this comparison, it must be considered that 1 L of water contains 55 mol under standard conditions, but 1 L of PFD contains no more than 4.2 mol.

The molecular ratio of dissolved oxygen in water compared to dissolved oxygen in PFD is 1_{O2} : 200_{H2O}, but 5_{O2} :1_{PFD}. This means a 1000× increased molecular O_2 solubility for PFD compared to water (**Figure 4**, used by permission (61)).

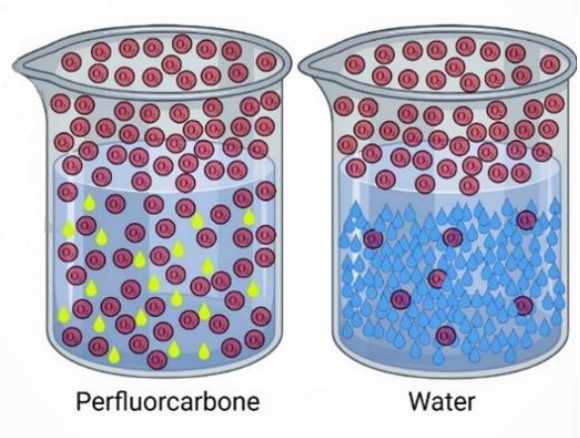

Figure 4. Comparison of the O_2 capacity of water and PFC at the same pO_2.

Because of their chemical and metabolic inertness, PFCs produce no toxic degradation products (64). There are two more characteristics that make PFCs ideal candidates for DCI prevention and treatment: their ability to enhance oxygen delivery combined with the facilitation of nitrogen bubble elimination (65). Nitrogen solubility at 25°C in *Oxycyte*®, a third-generation 60% PFC emulsion, reaches 22 ml N_2 / 100 ml PFC (66). *Yoshitani et al.* could show that size and quantity of nitrogen bubbles were reduced by PFC in a cardiopulmonary bypass model (67). Another effect of PFC is their ability to act as a surfactant: the adhesion of bubbles to the endothelium is hampered and thrombin production reduced (10,68).

A basic problem is the creation of PFC preparations that allow intravenous administration. Important parameters in this context are their retention time in the vascular system, their organ retention time and emulsifiability. Particularly suitable are, for example, perfluorodecalin (C10F18), perfluoroctylbromide (CF3(CF2)7Br), and perfluorotert-butylcyclohexan (C10F20).

1.5. **Perfluorocarbons for intravenous use**

Intravenous application of unprocessed PFC results in life-threatening intrapulmonary foam formation (69). Emulsification is necessary because PFCs are neither hydro- nor lipophile and therefore immiscible with aqueous fluids like blood. Only small amounts of PFC molecules are tolerated in the blood stream without serious consequences: Emulsion droplets are phagocytized and attached to lipoproteins, PFC molecules are then transported to the lung, where they can be exhaled, if they are characterized by high vapor pressure such as perfluorodecalin (60,64,70). A PFC with exceptional characteristics is dodecafluoropentane (DDFPe). Its boiling point of 29°C leads to volatilization at biological temperatures. The half-life of DDFPe in systemic circulation is extremely short and it is nearly completely exhaled by the lungs (71).

The formulation of a homogenous, sterile emulsion, which is stable at room temperature and characterized by a droplet size of 0.1 to 0.2 µm, is technically complex. *Ostwald ripening*, caused by molecular diffusion, results in enlargement of the droplets. This process can be counteracted by either adding a small amount of PFC with a higher molecular weight (unfortunately associated with longer organ retention time) or emulsifiers to reduce surface tension (72). Highly effective synthetically produced emulsifiers can lead to severe side-effects (73,74). PFC emulsions of the last generation are based on the combination of different emulsifiers such as more tolerable but less stabilizing phospholipids (e.g. egg yolk) with PFCs like perfluorotributylamine (N(CF2CF2CF2CF3)3) or perfluoromethylcyclo-hexylpiperidin (C12F22N) (73,74). High molecular weight PFCs, as the latter, are characterized by long persistence in organs resulting in negative decisions from regulatory authorities.

Thus, there is a clear need for the development of non-toxic PFC-formulations which can be stored easily and administered intravenously. An alternative option to guarantee a stable formulation without *Ostwald ripening* and the disadvantage of prolonged elimination time is the encapsulation of PFC with polymers, for example poly(lactide-co-glycolide) (75,76) or poly(n-butyl-cyanoacrylate) (77,78). Such nanocapsules with a polymer-based shell can be used for controlled drug delivery (79-82) and artificial oxygen carriers (77,78,83). Compatibility with aqueous medium blood and the exchange of respiratory gases is enabled through the thin capsule wall (77). However, not every kind of shell material is suitable. Poly(n-butyl-cyanoacrylate), for example, is associated with insufficient biocompatibility (78).

The intensive search led to a combination of the amphiphilic biopolymer albumin, which is characterized by lacking toxicity and antigenicity (84), with PFD comprising a PFC particularly

suitable for medical purposes. The resulting albumin-derived artificial oxygen carriers (A-AOCs) revealed a higher oxygen transport capacity than Perftoran® with tolerable side-effects (85). **Figure 5** shows a schematic illustration of an albumin-derived perfluorocarbon-based artificial oxygen carrier with an albumin shell containing the structure of perfluorodecalin (PFD).

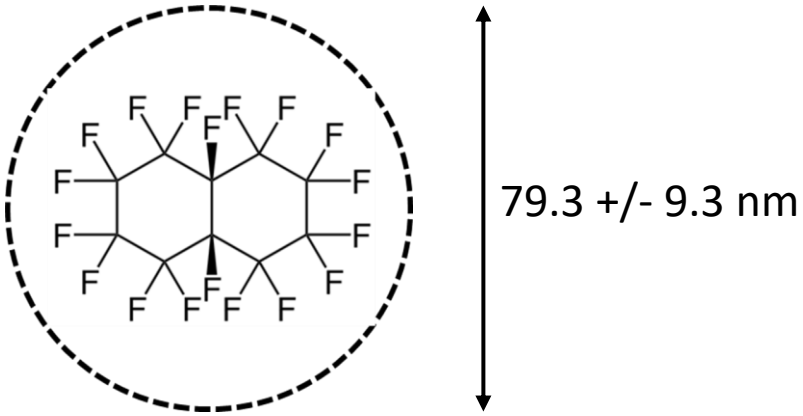

Figure 5. Albumin-derived perfluorocarbon-based artificial oxygen carrier.

1.6. **Perfluorocarbon-based preparations in the treatment of DCS**

Table 1 provides an overview of at least temporarily commercially available PFC-preparations, their main reasons for rejection by official authorities, preclinical and clinical studies (modified from (86)).

Table 1. PFC-preparations and main reasons for rejection by official authorities.

Product name	Company	PFC-composition	Emulsifier	Mean droplet size	Storage	Reasons for missing approval	(pre-) clinical studies
Fluosol-DA® (FG)	Fluosol-DA, Green Cross Corp., Osaka, Japan; Alpha Therapeutic, Los Angeles, CA, USA	14% perfluoro-decalin, 6% perfluoro-tripropylamine	Pluronic F-68, egg yolk-phospho-lipids, potassium oleate	0.12 µm	frozen	Insufficient stability, long organ retention time of 65 days	(64, 87-89)*, (90-92)**
Oxypherol® / Fluosol-43T® / FC 43® (FG)	Fluosol-DA, Green Cross Corp., Osaka, Japan; Alpha Therapeutic, Los Angeles, CA, USA	20% perfluoro-tributylamine			not known	Extremely long organ retention time, half-life in the rat about 2.5 years	(48, 93-96)*
Perftoran® / Vidaphor® (FG)	FluorO2 Therapeutics, Boca Raton, Florida. Ftorosan, OJCS SPF Perftoran Russian, Moscow, Russia	1% perfluoro-decalin, 3% perfluoro-methylcyclohexyl-piperidin	Proxanol 268, egg yolk-phospho-lipids	0.03–0.15 µm	3 years frozen (-4 to -18°C)	Long organ retention time of 90 days (approval only in Russia, Ukraine, Kazakhstan Kyrgyzstan, Mexico)	(97, 98)*, (99)**
Oxygent® (SG)	AF0144, Alliance Pharmaceutical Corporation, San Diego, CA, USA; Double Crane Pharm. Co., Beijing, China	58% perfluor-. octylbromide, 2% perfluoro-decylbromide	egg yolk-phospho-lipids	0.16 µm	1-2 years, 5-10°C	Severe side effects such as ileus and increased frequency of strokes	(65, 100-102)* (103-105)**
Oxycyte® (SG)	Tenax Therapeutics, Inc., Morrisville, NC (Synthetic Blood Int. Inc.)	60% perfluoro-Tertbutylcyclo-hexan	egg yolk-phospho-lipids	0.2 µm	not known	Sponsor withdrew support	(67, 106)*, (107)**
Oxyfluor® (SG)	HemaGen Inc, St. Louis, MO	78% perfluoro-dichlorooctane	egg yolk-phospho-lipids, safflower oil		1 year, room temp.	Phase III clinical trials suspended	(108, 109)* (107)**

*FG = First generation PFC, SG=Second generation PFC, *preclinical studies, **clinical studies, or summary*

1.6.1. **Preclinical studies**

Lutz et al. and *Lynch et al.* reported for the first time a life-prolonging effect of PFC in simulated air dives (89,96). In 1988 *Spiess et al.* demonstrated that after diving rats treated with Fluosol-43® in combination with 100% oxygen survived longer and showed less neurologic deficits compared with a control group treated with 6% hydroxyethyl starch (48). The same

working group found a significant survival benefit for rabbits in the PFC pre-treated group after triggering venous gas embolism, indicating gas absorptive properties of this substance (93). It took until the 90s before experiments using *Oxygent*® (at that time developed by *Alliance Pharmaceuticals Inc*, San Diego, California, presently marketed by *Beijing-DoubleCrane Pharmaceuticals*, China) delivered new findings in a swine-model confirming a dramatic reduction in DCI-lethality. *Dromsky et al.* examined for the first time the treatment potential of perflubron emulsion combined with 100% inspired O_2 in a large-animal model. Surgical catheterization of a peripheral vein before the dry chamber dive allowed i.v. application of *Oxygent*® immediately after decompression. PFC decreased and delayed the onset of cardiopulmonary DCI and prevented neurological symptoms (100). A protective effect of PFC in a dog model of AGE was associated with a lower risk of cerebral strokes and improved cerebral blood flow (110). Several studies in animal models with VGE and AGE consistently showed the resorptive capabilities of PFC (67,109,111). In a dog model, an infusion of a perfluorodecalin-glycerol emulsion was able to enhance the off-gassing of xenon from muscle tissue (112). Using a Russian preparation (*Perftoran*®), *Eckmann et al.* demonstrated a protective effect of PFC against air bubble damage in cultured endothelial cells (97). Further studies in rabbits showed that PFC promotes the pulmonary elimination of nitrogen and, thus, increases the elimination of the bubbles (65).

The second main effect of DCS-therapy was described in sheep-experiments entailing application of perfluorotertbutylcyclohexan showing an increase in oxygen-delivery to and -utilization in ischemic tissues (106). For the optimization of DCS therapy, the correct time frame of PFC application appears important. In a study of *Dainer et al.* in a swine-model, preventive administration of PFC at depth before decompression did not lead to better results; best efficacy was achieved by administering PFC after diving with 100% oxygen breathing content (102). *Mahon et al.* tested the efficacy of *Oxygent*® in combination with oxygen with an application time lag following the onset of DCS demonstrating that even delayed administration of PFC is effective in decreasing mortality in a swine model (101).

But not every PFC preparation improves DCS mortality. *Sheppard et al.* showed in a rat model with DCS that the use of dodecafluoropentane (DDFPe) is associated with high mortality and lack of beneficial effects (56). According to *Randsoe et al.* under normobaric conditions, the combination of breathing oxygen and PFC leads to accelerated reduction of bubbles and both therapies complement each other (113). The initial bubble growth caused by increased oxygen tension is only transient and compensated by the passive transport capacity of PFC. However, the additional use of a hyperbaric chamber to further boost the positive effect of PFCs

was of no further benefit. Furthermore, the combination of breathing highly concentrated oxygen with PFC as a substance with high oxygen capacity appears to be dangerous at depth. *Mahon et al.* showed in a swine-model at 507 kPa a significant increase of seizures versus the control group with saline infusion (114). Further studies are necessary to assess if a combined PFC-oxygen-therapy at lower pressures can avoid toxic oxygen-effects with higher efficacy than PFC alone (see 1.6.2. risk of seizures).

Keipert et al. described a febrile reaction up to 1-1.5 °C of 6 to 8-hour duration in rats after intravenous application of a concentrated emulsion of *Oxygent*®. Intensity and duration of the fever attacks showed inverse dependency on particle size. The authors concluded that emulsion particles < 0.2 µm are associated with a longer half-life persistence in blood, less activity of macrophages and thus reduced temperature response (115).

Intravenous infusion of nanocapsules with a polymer-based shell, for example poly(lactide-co-glycolide) or poly(n-butyl-cyanoacrylate) are in general well tolerated by animals, but side-effects can occur, e.g., transient decrease in mean arterial blood pressure, impairment of hepatic microcirculation, organ/tissue damage of liver, spleen and small intestine, elevation of plasma enzyme activities such as lactate dehydrogenase, creatine kinase and aspartate aminotransferase. Although the organ most affected depends on the shell material used, accumulation of polymer-based shell nanocapsules can be assumed in the spleen, kidneys and small intestine (78). The development of more suitable shell materials should combine the favorable gas exchange properties of PFC-nanocapsules with a low risk of potential long-term toxicity.

1.6.2. **Perfluorocarbon-based preparations in clinical trials**

Although the physico-chemical properties of PFC-based preparations appear to make them ideal candidates for DCI therapy and many preclinical studies apparently confirm this concept, until today, no broad success in clinical practice has been achieved.

One fundamental and recurrent problem of PFC emulsions is their long organ retention time which can be associated with an incalculable long-term effect. Further development of *Oxypherol*®, a stable emulsion based on a combination of perfluorotributylamin with *Pluronic F-68* was discontinued for this reason (116). *Perftoran*® is the only PFC preparation with limited approval by official authorities in Russia, Ukraine, Kazakhstan, Kyrgyzstan, and Mexico (86). Main indications are acute blood loss, improvement of oxygenation of specific tissues for example in coronary heart disease, ischemic disorders of extremities and brain, acute

or chronic anemia and wound healing (99,117). *Perftoran*® is generally well tolerated; rarely occurring side-effects are dizziness, kidney pain, hypotension, hyperemia, lung symptoms and temporary itching (99). Its long organ retention time (90 days) caused by the additive of perfluoromethylcyclohexylpiperidine (86) a and non-conform production process, resulted in refused approval of *Perftoran*® in Europe and USA. Currently, there are efforts to produce *Perftoran*® under good clinical practice conditions and thus to gain U.S. Food and Drug Administration approval under the brand name *Vidaphor*® (118).

Other problems are instability and cumbersome handling of the PFC emulsions. In the early 1990s, *Fluosol-DA*® was officially accepted for improving oxygenation during coronary angioplasty in USA, Europe, and Japan (63,70,86,119). Mainly because of its instability and long organ half-life the approval was withdrawn a few years later. The substance is difficult to handle, it requires storage at -20 degree Celsius and a long defrosting period (64). In 1994, the production of *Fluosol-DA*® was suspended (63).

A new generation of PFC-products allowed storage without freezing and 2 to 4 times higher PFC contents by using natural phospholipids as emulsifiers (86). In phase-II-studies *Oxygent*® showed positive effects in patients with cardiac surgery and orthopedic interventions combined with hemodilution (86, 120). Two phase-III-studies in Europe, USA and Canada reported less transfusions but also severe side-effects such as post-surgical ileus and an increased frequency of strokes. A post-hoc-analysis could not confirm this association, but the sponsor stopped the study (105). In 2005, another study with *Oxygent*® in cardiac surgery patients investigating brain circulation found increased neurological complications such as cerebral emboli. However, the detection technique was based on ultrasound Doppler, which could be a limitation in this setting and responsible for the negative outcome in the *Oxygent*®-treated patients (121). Since 2017, *Oxygent*® is approved in China for clinical studies in humans, financed by *Double Crane Pharm. Co.* (Beijing, China) (122,123).

In 2009, another PFC preparation *Oxycyte*® was tested in a phase-II-study including patients with severe traumatic brain injury. The study had to be terminated by the sponsor in 2014, due to problems with patient recruitment. The support of the product was withdrawn by the sponsor (107) and since then no other study with this PFC emulsion has been published.

The extremely high gas-dissolving capacity of PFCs could be associated with an increased risk of seizures due to toxic oxygen effects, especially if PFCs are combined with hyperbaric oxygen. In a recent study, *Cronin et al.* found no increased rate of seizures in swine treated with PFC followed by recompression with hyperbaric oxygen (124).

Several study groups have described increasing pulmonary arterial pressure (PAP) after application of PFC in various species (106,125,126). This effect could be highly relevant, because severe DCS itself can cause high PAP due to mechanical obstruction by nitrogen bubbles or indirectly by endothelial effects leading to vasoconstriction (56,127). *Mahon et al.* found a prolonged PAP increase in a mixed-sex swine study using the emulsified perfluorocarbon *Oxycyte*® (128). An adverse pulmonary reaction has been described after the application of the PFC preparation *Fluosol*® in humans (90). This dangerous effect could be caused by the retention of lipid particles > 0.35 µm in the lung with consecutive activation of the complement system called complement activation pseudoallergy (CARPA) (56, 129). PFC-emulsions like *Oxycyte*® with a particle size up to 0.6 µm (median size 0.2-0.25 µm) could trigger CARPA. It has to be considered that nanocapsules-based PFC preparations like A-AOCs, characterized by a mean diameter of 0.4 up to 0.7 µm (85), could also lead to an increase of PAP in association with CARPA.

Figure 6 (used by permission (61)) gives an overview of possible interaction of PFCs with tissue and blood. In spite of the fact that PFCs are inert, there are relevant interactions, e.g., with the lipid bilayer of cell and different organelle membranes (**A**) (130). The deposition of PFCs inside the *Kupffer cells* is associated with a foamy appearance (**A**) (131). CYP450 monooxygenase is inactive due to lack of reduced coenzyme NADPH. Reduced coenzyme $NADH+H^+$ is also decreased. Therefore, oxaloacetate cannot leave mitochondrion and glucogenesis is not possible. Inactivation of CYP450 monooxygenases reduces the hepatic detoxification ability. (**B**) (132-135). Phospholipid-wrapped PFCs and natural lipid vesicles may fuse and form hybrid vesicles (**C**) (136,137). PFC droplets are opsonized by complement factors or antibodies to be recognized and phagocytized by macrophages (**D**) (138).

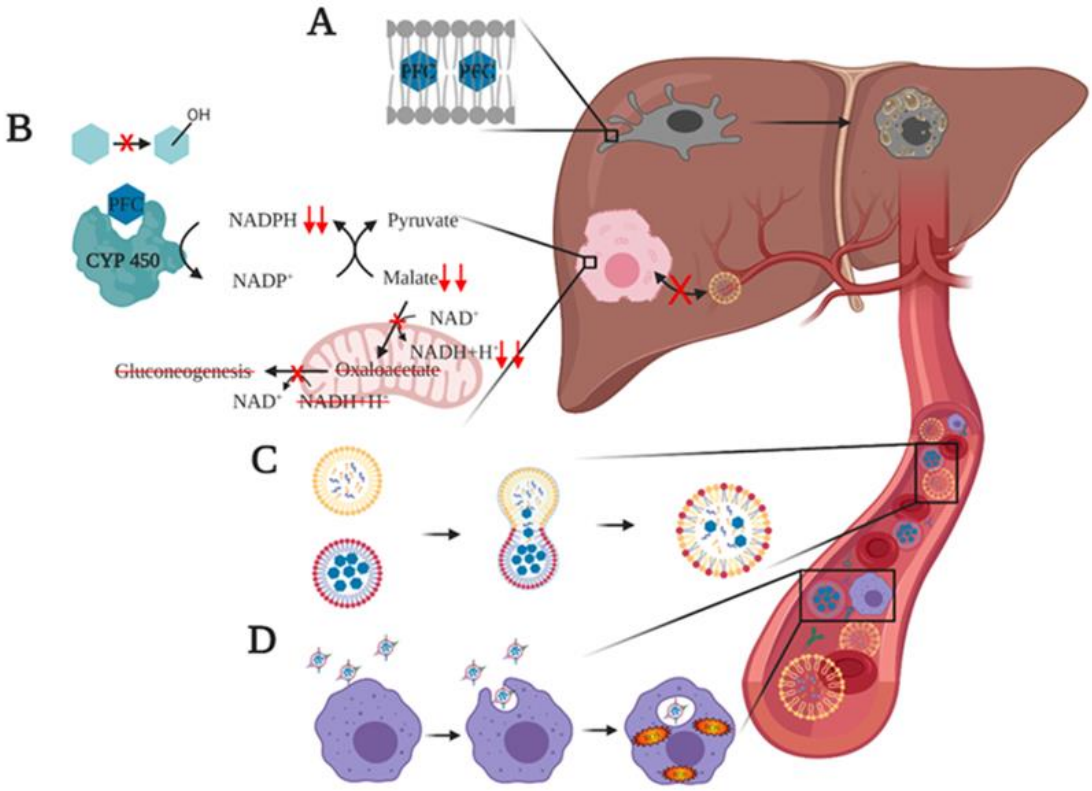

Figure 6. Interaction of PFCs with tissue and blood.

1.7. **Albumin-derived artificial oxygen carriers as a new concept**

Originally, albumin-derived artificial oxygen carriers (A-AOCs) were developed as artificial oxygen carriers based on nanocapsule technology with properties in terms of biocompatibility and gas exchange comparable to emulsions (85, 139). The synthetic procedure entails using ultrasound in the presence of albumin. Amphiphilic albumin as shell material encloses a core of PFD, thus avoiding the requirement of an additional emulsifier. In vitro tests have shown effective oxygen transport capacity of A-AOCs (85), further supported by the proof of functionality in the *Langendorff-heart-model* (139) and also in vivo studies of the rat regarding toxicity and pharmacokinetics (140). Intravenous application of A-AOCs was well tolerated in rats with stabile vascular perfusion and without change in systemic parameters. There was no indication of relevant tissue injury and the half-life of A-AOCs (158 min) was sufficient (85). An in vivo proof-of-concept-study then demonstrated survival of rats after progressive exchange of 95% of blood with A-AOCs (140).

The underlying concept of the study described here is the elimination of nitrogen bubbles based on the permeability of the nanocapsules' shell-material and the gas exchange capacity of PFC. The ability of fluorinated hydrocarbons to increase oxygen delivery to tissues combined with rapid dissolvement and transport of N_2 from tissues to the lungs offers the possibility to prevent the formation of N_2 gas emboli. Furthermore, there is some evidence for stabilization of nitrogen bubbles by nanoparticles based on the *Pickering effect* (**Figure 7**) (141,142). It is assumed that nanocapsules cover the surface of small nitrogen bubbles in the nascent state and stabilize them in aqueous dispersion. Hereby, they can prevent further agglomeration and subsequent growth of the bubbles and enable their effective transport in the blood plasma. In this way, the *Pickering effect* adds to the beneficial capability of the A-AOCs to carry nitrogen in the dissolved state and explains the reduced expression of decompression illness observed also after application of PFC-free oil-filled nanocapsules (143).

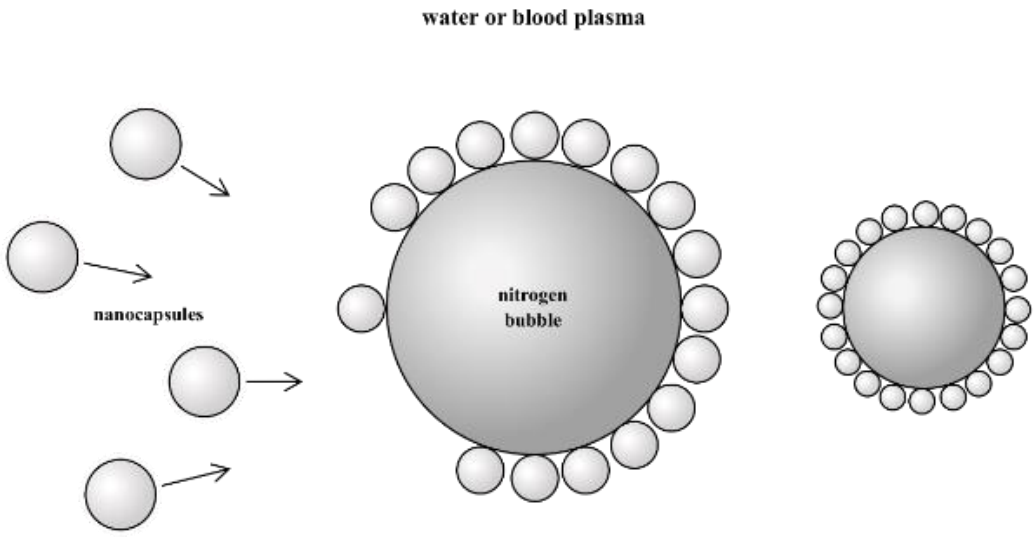

Figure 7. Pickering effect.

Figure 8 demonstrates the ability of PFC containing nanocapsules to capture nitrogen from bubbles adherent to the endothelial wall and to transport it to the lungs, where it is exhaled. Oxygen is transported from the lung to putatively hypoxic regions like small vessels and capillaries.

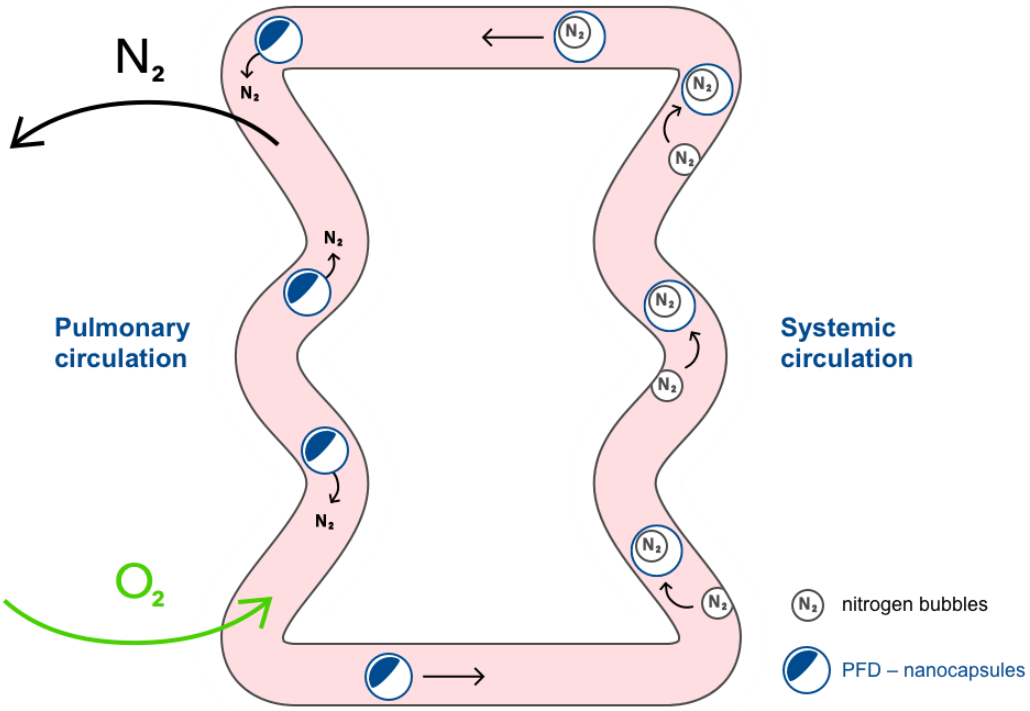

Figure 8. Transport of nitrogen to the lungs by PFD-nanocapsules.

2. AIM OF THE STUDY

In a rodent in-vivo model we investigated the effect of a nanocapsules-based PFC preparation on DCS expression. The aim of the present study was to examine different parameters (clinical presentation, serological, macroscopic, and histologic alterations) after a simulated dive with an increase in the surrounding pressure, followed by decompression back to normal atmosphere according to a defined diving protocol.

We hypothesize that intravenous administration of A-AOCs before decompression will improve the survival rate and reduce decompression related symptoms in rats compared to a group of animals receiving nanocapsules containing a neutral oil and a third group treated only with an albumin injection. An additional control group received A-AOCs without following hyperbaric exposure.

3. METHODS

3.1. Materials

Albunorm®, a plasma-like solution containing 5% human serum albumin, 0.75% NaCl, 0.11% sodium-N-acetyltryptophanoate, and 0.07% sodium caprylate was purchased from *Octapharma* (Langenfeld, Germany). Perfluorodecalin (PFD) was obtained from *Fluorochem Chemicals* (Derbyshire, UK). *Miglyol 812®* was purchased from *Caelo* (Hilden, Germany), Glycerin was purchased from *Carl Roth* (Karlsruhe, Germany).

3.2. Synthesis of nanocapsules

The synthesis of nanocapsules was performed as described previously (85) with slight modifications. The production took place 3-6 days prior to use in the animal experiments. In detail, 10 ml *Albunorm®* and 2 ml PFD (for A-AOCs) or 2 ml of neutral oil (*Miglyol®*) mixed with glycerin 1:1 (for albumin-derived neutral oil-based nanocapsules, A-O-N) were combined in a reaction tube with a total capacity of 50 ml. The reaction tube was cooled in an ice bath (-20°C) while sonicating the mixture. Using a sonotrode with a tip diameter of 14 mm associated with a UP 400St ultrasonic processor (*Hielscher*, Teltow, Germany) the mixture was treated with an energy input of 8100 Ws and an amplitude of 40%. For sonication, the tip of the sonotrode was placed at the PFD–water interface. After synthesis, capsules were adjusted to 17 vol% (for A-O-N) or 55-64 vol% (for A-AOCs) using microhematocrit glass capillary tubes (d = 1.15 mm, *Brand*, Wertheim, Germany) and a centrifuge (*Universal 320R*, *Hettich*, Tuttlingen, Germany) with a hematocrit rotor.

To achieve 55-64 vol% (for A-AOCs), capsules were centrifuged in 50 ml reaction tubes twice for 20 minutes at 1500 rpm respectively 3000 rpm (*Biofuge primo R*, *Heraeus*, Hanau, Germany). After removing the supernatant, the pellets were resuspended to reach the desired concentration of A-AOCs. Concentration of A-O-N was technically not possible because of the minimal difference in density.

3.3. **Determination of size of nanocapsules**

To ensure comparable particles for injection in every animal, the radii of A-O-Ns and A-AOCs were monitored during and beyond the experimental period using dark field microscopy: Brownian motion of the nanocapsules was tracked online and used for calculation of particle size as described previously (144) using *ANT2013* software. Samples were diluted with water (1:50) and observed using an *Orthoplan* microscope (*Leitz*, Wetzlar, Germany) equipped with a PL-40 objective and a charge-coupled device (CCD) camera. Measurements (n=10 per group) were performed 1, 4 and 8 days after synthesis at room temperature with a film thickness of 3 µm. Due to different optical properties, parameters for A-AOC measurements / A-O-N measurement, respectively, for *ARNT-2013* software were set as follows: brightness threshold 130/140, minimal radius expected 50/50, minimal number of pixels 30/30, number of images per sequence 100/300.

Mean hydrodynamic radii of A-AOCs and A-O-Ns remained constant around 80 nm and 200 nm, respectively, throughout the experimental period that was 3-6 days after synthesis. In detail, radii for A-AOCs were 79.30 nm +/- 9.30 nm (day 1), 80.80 nm +/- 12.96 nm (day 4), 79.50 nm +/- 7.63 nm (day 8) while A-O-Ns were larger with 211.50 nm +/- 36.13 nm (day 1), 203.20 nm +/- 29.83 nm (day 4) and 201.50 nm +/- 17.48 nm (day 8), respectively.

3.4. **Animal experiments**

All experiments were approved by local *French ethical comity* (*CEFEA*, n°74), and authorized by the French "Ministère de l'Éducation Nationale, de l'Enseignement Supérieur et de la Recherche et de l'Innovation" under the number APAFIS#16520-18082715001698v4. Sixty male Wistar rats (weight: 318 – 430 g, 11 weeks old on the day of the experiment) were obtained from *Janvier SAS* (Le Genest St Isle, France). The rats were housed in the university vivarium for at least 7 days after arrival, two per cage under controlled temperature (21 ± 1°C) and lighting (12 h of light per day, 8.00–20.00). Animals were fed standard rat chow (*Kliba Nafag*, M/R Maintenance, 3.152 kcal/g). Water and food were supplied ad libitum.

The animals were randomly assigned into 4 groups. In each group, 15 rats were included. **Figure 9** shows the time chart of the experimental set-up. At the beginning (time point 0 min) the tails of the rats were anesthetized with xylocaine (*Anesderm*® Gé, 5%) and the animals were immediately put under a heat lamp for at least 20 minutes to achieve increased blood flow of the tail vein. Then they received gaseous anesthesia with isoflurane

(4.0% in 100% medical O_2 at 2.0 l/min) through face masks for 5 minutes before injection of 1 ml of the test substance via the tail vein using a 25 G cannula (time point +25 min) (**Figure 10**).

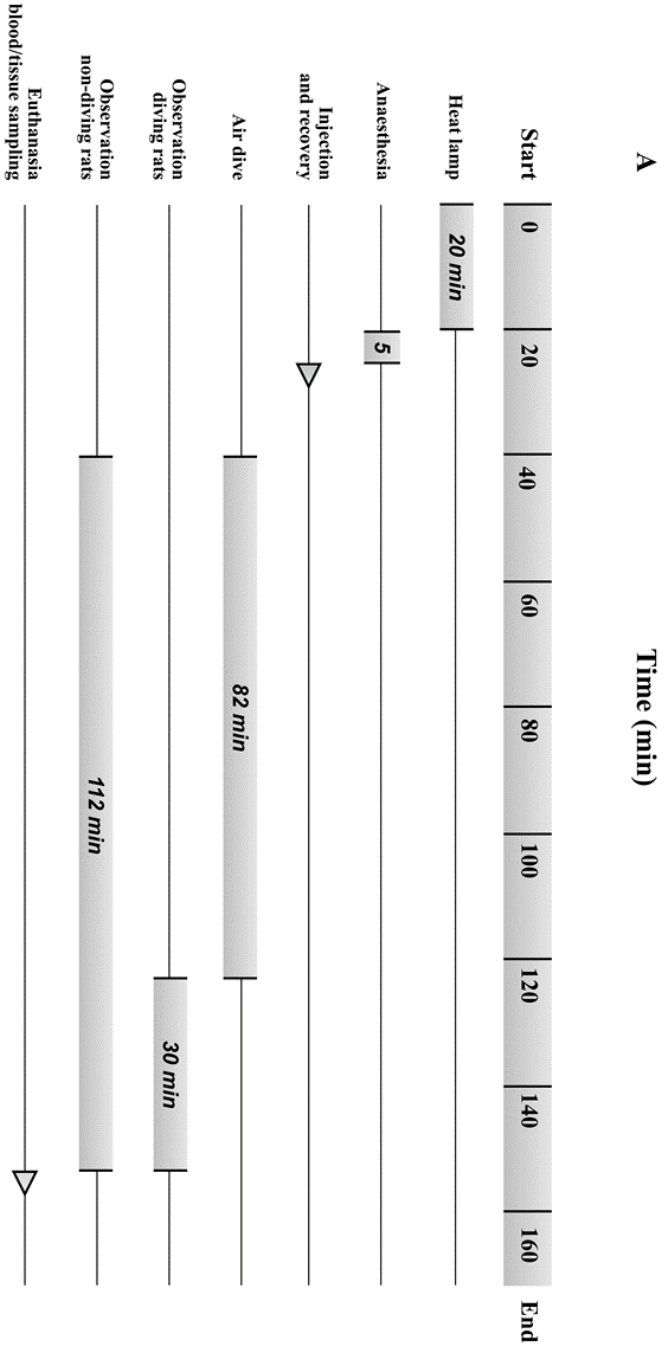

Figure 9. Time chart of the experimental set-up.

Figure 10. Injection of the test substance via the tail vein.

A total of 12 animals had to be excluded from the study because of failed or incomplete injection of the test substance in the tail vein (group 1: n=3, group 2: n=3, group 3: n=2, group 4: n=4). Successful injection was verified at the end of the experiment by a white pellet (= nanocapsules) in the blood sample collected for plasma analysis (**Figure 11**).

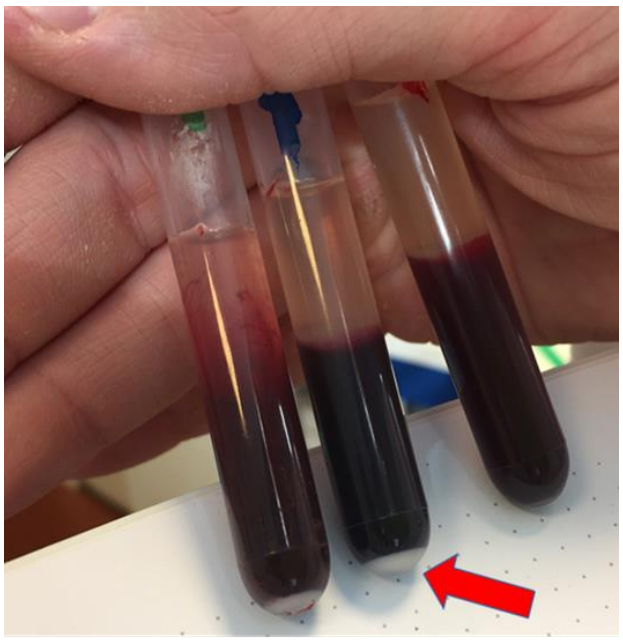

Figure 11. Two glass containers on left show precipitation of nanocapsules.

3.5. **Test groups**

Group 1 (A-AOCs-dive, n=12): Experimental group. Rats subjected to a simulated dive to 90 meters, with preceding injection of A-AOCs (1 ml, dispersed in *Albunorm*®).

Group 2 (A-O-N-dive, n=12): Experimental group. Rats subjected to a simulated dive to 90 meters, with preceding injection of Albumin-derived neutral oil-based nanocapsules (A-O-N) (1 ml, dispersed in *Albunorm*®).

Group 3 (A-0-0-dive, n=13): Experimental group. Rats subjected to a simulated dive to 90 meters, with preceding injection of only *Albunorm*® (A-0-0) (1 ml) without nanocapsules.

Group 4 (A-AOCs-surface, n=11): Control group. Non-diving rats with preceding injection of A-AOCs (1 ml, dispersed in *Albunorm*®).

3.6. **Hyperbaric protocol**

At time point +40 min, the animals of the experimental groups 1-3 were exposed to the simulated dive, each rat housed in single cages. At that time point, all animals were awake again and showed normal behavior. Each rat was positioned in a 130L steel hyperbaric chamber in Francois Guerrero´s laboratory at the University of Brest (**Figure 12**). Air was used as a breathing mixture. Compression took place with air at a rate of 100 kPa/min up to 1,000 kPa absolute pressure (90 meters of sea water, msw) and remained at maximum pressure for 35 min. Thereafter, decompression was performed at a rate of 100 kPa/min before pausing for three decompression stops: 5 min at 200 kPa (10 msw), 5 min at 160 kPa (6 msw), and 10 min at 130 kPa (3 msw). Total hyperbaric exposure duration was 82 min. All dive depths were monitored using a modified personal dive computer (Puk; Mares, Rapallo, Italy). Animals were brought out of the chamber at time point +122 min. **Figure 13** shows the time chart of the simulated diving profile.

Figure 12. Opened 130-l steel decompression chamber.

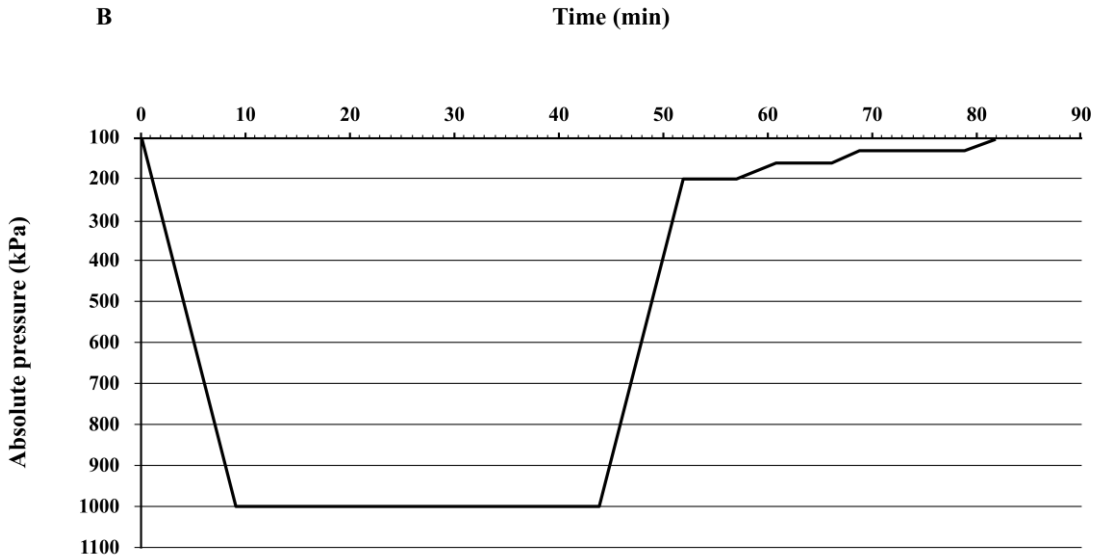

Figure 13. Time chart of the simulated diving profile.

3.7. **Clinical observation following decompression**

Following decompression, the rats of the groups 1-3 were observed for 30 minutes regarding the appearance of DCS. Animals were scored as having DCS only when displaying one or more symptoms of respiratory distress, difficulty walking, paralysis, or convulsions (145). The classification of DCS and the analytical method were decided a priori to the experiment. To minimize the potential for animal suffering, a pain/distress scale was approved by the *Animal Research Ethics Committee* and no rats displayed signs of distress at or above the level where early euthanasia was required. In this study, the ternary classification of "No DCS" (no symptoms), mild "DCS" (with at least one symptom excluding death within the observation period) or severe DCS ("Death" within the observation period) was applied to maximize statistical power, as described by *Buzzacott et al.* [29]. Animals which did not present symptoms of DCS were euthanized at the end of the 30 minutes observation period (time point +162) for tissue sampling.

The non-diving rats of group 4 were similarly confined but without exposure to pressure and were observed for 112 minutes before physiological investigation.

Additionally, the survival time of each animal was measured. Survival time was defined as the time period of surviving after opening the chamber at the end of the hyperbaric procedure. If the animal was dead when the chamber was opened (time point + 122 minutes) survival time was defined as 0 minutes. If the animal died during the 30 minutes observation time, the time period until its death was measured in minutes. If the animal survived for at least 30 minutes the survival time was defined as 30 minutes or 100 %. Therefore, a mean survival time of 30 minutes for a group means that all animals survived all the observation period. Conversely, if only one animal died before the end of the observation period, the mean survival time of the group was different (less) than 30 minutes or <100%.

3.8. **Blood sampling**

After diving simulation and subsequent observation, the animals were anesthetized with Ketamine (*Ketamine 100, Virbac*, 80 mg/kg) and Xylazine (*Rompun 2%, Bayer*, 12 mg/kg) injected via intraperitoneal injection. Intracardiac blood collection was performed immediately following anesthesia in several 2 ml Eppendorf tubes with 30 µl of 5% EDTA as an anticoagulant. Blood was centrifuged at 1,400 G and 20°C for 15 min. Collected plasma was aliquoted and stored at −80°C until further analysis.

3.9. **Determination of plasma parameters**

The plasma activity of lactate dehydrogenase (LDH, U/L) as a general marker of cell injury, creatine kinase (CK, U/L) as a marker for muscle cell injury, aspartate aminotransferase (ASAT, U/L) and alanine aminotransferase (ALAT, U/L) as markers for hepatocyte injury as well as the plasma creatinine concentration (creatinine, mg/dL) as a marker of renal function were determined using a fully automated clinical chemistry analyzer (*Vitalab Selectra E, VWR International*, Darmstadt, Germany) and commercially available reagent kits (*DiaSys*, Holzheim, Germany) as previously described [27]. In addition, the following parameters were determined using the same analyzer: Complement 3c (mg/dL) as a major plasma protein of the immune system complement pathways, increased in response to inflammation; urea (mg/dL) as a marker for kidney function; Immunoglobulin M (IgM, mg/dL), an isotype that binds and activates complement; D-dimer (µg/mL), reflecting ongoing activation of the hemostatic system; P-Amylase (U/L) as a marker for pancreatic disorder. Myoglobin (ng/mL) is rapidly released after muscle damage and can be used as a biomarker in the early phases of injury. Because myoglobin has a short half-life of 2–3 hours and undergoes rapid renal clearance, changes in serum concentrations usually occur over a shorter time-course than do changes in serum levels of CK. Serum lactate levels (mg/dL) in circulation were measured as a quickly reacting marker for systemic tissue hypoperfusion and circulatory shock.

3.10. **Tissue sampling**

After completing blood sampling, rats were euthanized via intracardial punction. The thorax and abdomen were incised, and liver, spleen, intestine, kidneys, heart, and lungs were assessed macroscopically. Particular attention was given to oedema and gas content in vessels and intestine. Then organs were resected and weighed (total wet weight). Additionally, parts of lung and liver were weighed before and after drying to determine the dry/wet ratio. Brain, parts of lung, liver, kidney, heart, spleen were stored in 4% paraformaldehyde solution until further processing.

3.11. **Histological evaluation of organs**

Paraffin-embedded sections were stained with hematoxylin-eosin and evaluated in a blinded manner (5 image sections per tissue section). Spleen sections were assessed for integrity of red and white pulp. Kidney sections were assessed by scanning the renal tubules for vacuoles and the integrity of cell membranes and epithelium as well as by examining the glomeruli for swelling or shrinkage. Liver sections were assessed for integrity and vacuolization. All organ sections were investigated by light microscopy with a 200x magnification.

The severity of histological changes was assessed with modified *Suzuki's criteria* (146). In this modification, all histologic parameters were graded from 0 to 3 according to the degree of severity of the histopathological changes (0=no/minimal, 1=mild, 2=moderate, 3=severe changes of vacuolization, circulatory disorder, hepatocyte damage and width of sinusoids).

3.12. **Statistical analysis**

Statistical analysis was performed using MedCalc Statistical Software version 20.014 (*MedCalc Software bvba*, Ostend, Belgium; 2021).

Sample size calculation was based on a proportion for severe DCS of 64% according to *Lautridou et al.* 2017 (147) and personal communication with *Prof. F. Guerrero*. Setting significance threshold for a type I error at 0.05, and for a type II error at 0.20, a minimum of 12 animals had to be included into each group.

Results of clinical observation were evaluated with Chi square test, Kruskal-Wallis test, Mann-Whitney test, and logrank test (5% significance level).

For plasma marker analysis, upon identifying significant differences in the Kruskal-Wallis test, a Dunn's post hoc test was used to investigate the relevant parameters. For the nonparametrically distributed results, we ran Kruskal-Wallis and Mann-Whitney tests. Significance was accepted at $p \leq 0.05$. Results are expressed as means with 95% confidence interval (CI), and medians with 95% CI or interquartile range (IQR); n indicates the number of rats.

4. RESULTS

4.1. Occurrence and severity of DCS

The symptoms after animals' exposure to hyperbaric environment and following decompression were categorized according to a trinary classification (DCS-free, mild DCS with at least one symptom excluding death and severe DCS resulting in death within the observation period). The animals that died inside the chamber could not be observed before their death. The registration of typical DCS symptoms was only possible after the opening of the chamber. So there is no statement concerning symptoms for 8 animals of the A-0-0 group and 3 animals of the A-O-N group that were found dead in the chamber after decompression.

Table 2: Description of DCS symptoms.

	n	**no symptoms**	**respiratory distress***	**difficulty walking***	**paralysis***	**convulsions***	**death in chamber**	**death total**
A-AOCs-dive	12	9	2	1	0	1	0	1
A-O-N-dive	12	7	1	1	1	1	3	4
A-0-0-dive	13	2	1	1	1	0	8	9

*combination of different symptoms for one animal is possible

A-AOCs showed significant efficacy in reducing the symptoms of DCS. The occurrence and severity of DCS depended on the treatment group ($p=0.001$). DCS ratio was significantly lower in the A-AOCs group than in the A-0-0-dive group: nine A-AOCs-animals (75%) showed no DCS at all compared to 2 (15%) animals of the A-0-0-dive group ($p=0.002$). The DCS outcome was not significantly different in the A-O-N-dive group compared to the A-AOCs-dive group or the A-0-0-dive group. A-AOCs-dive animals were not significant different in DCS symptoms compared to non-diving controls (A-AOCs-surface), whereas A-O-N-dive animals differed significantly from A-AOCs-surface animals ($p=0.039$). A-0-0-dive animals also showed a significant difference to the A-AOCs-surface group ($p<0.001$) (**Figure 14**).

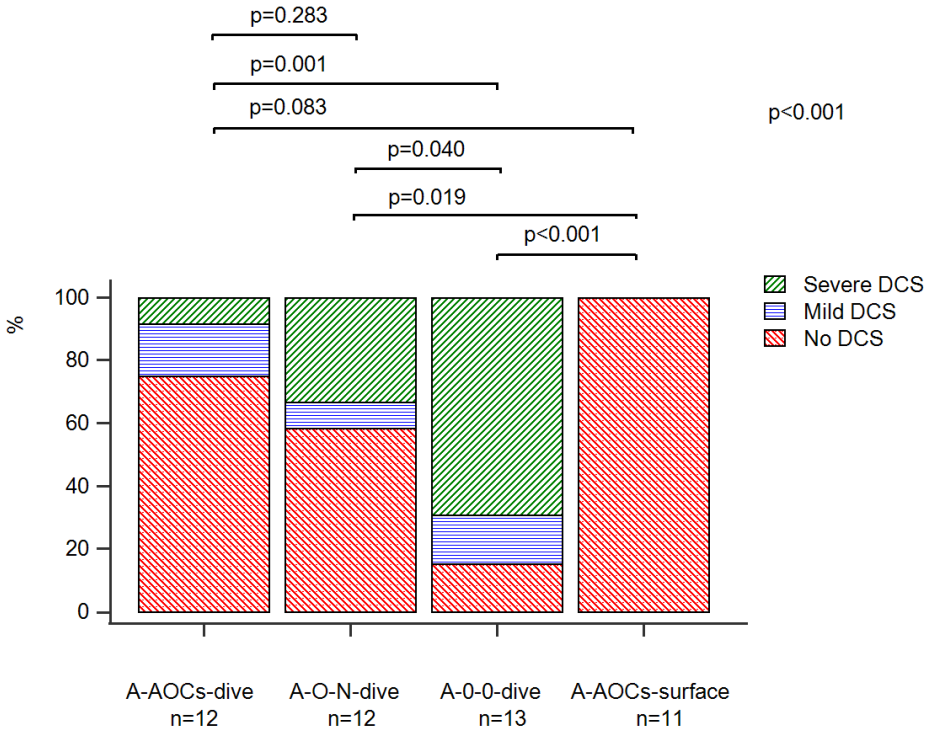

Figure 14. Occurrence of 3 levels of DCS.
Results of Kruskal-Wallis and Mann-Whitney test. *Mild DCS* at least one DCS symptom excluding death; *Severe DCS* death within the observation period

4.2. **Survival in DCS**

Pre-dive treatment with A-AOCs significantly prolonged the survival time of the animals after decompression (p=0.001). The difference between A-AOCs-dive and A-0-0-dive was statistically significant (p=0.001), marked with * (**Figure 15**).

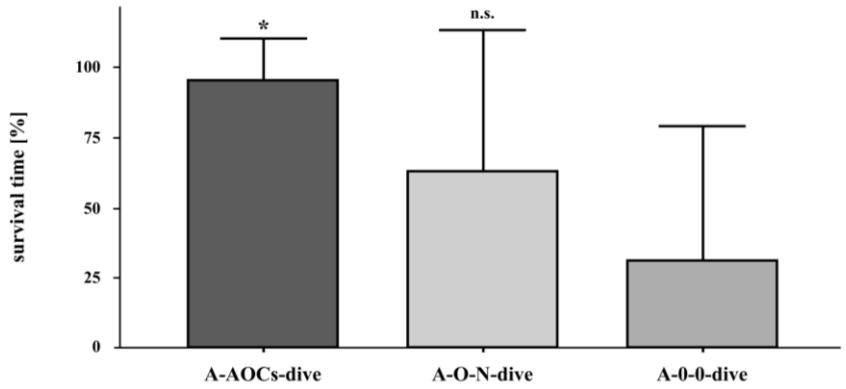

Figure 15. Survival time.
Arithmetic means and 95% confidence intervals of the arithmetic means, presented as proportions of the 30 minutes observation period beginning at the opening of the compression chamber.
Results of Mann-Whitney test. * Significant difference between A-AOCs-dive and A-0-0-dive (p=0.001). *n.s.* No significant difference between A-O-N-dive and A-AOCs-dive (p=0.103), and A-0-0-dive (p=0.069), respectively.

Survival probability was significantly higher in the A-AOCs-dive compared to A-0-0-dive animals (p=0.002), but not significantly different in the A-AOCs-dive group compared to the A-O-N-dive group (p=0.122) and even compared to the non-diving A-AOCs-surface group (p=0.338). There was a significant reduction of survival in the A-O-N-group compared to the A-AOCs-surface-group (p=0.039) (**Figure 16**). The character ↓ indicates the timepoint of leaving the decompression chamber. Animals in the control group, treated with A-AOCs without simulated diving (A-AOCs-surface), failed to exhibit any toxic side effects like change in behavior, respiratory distress, neurological deficits, or central reactions of the cardio-vascular system during an observation time period of 115 minutes.

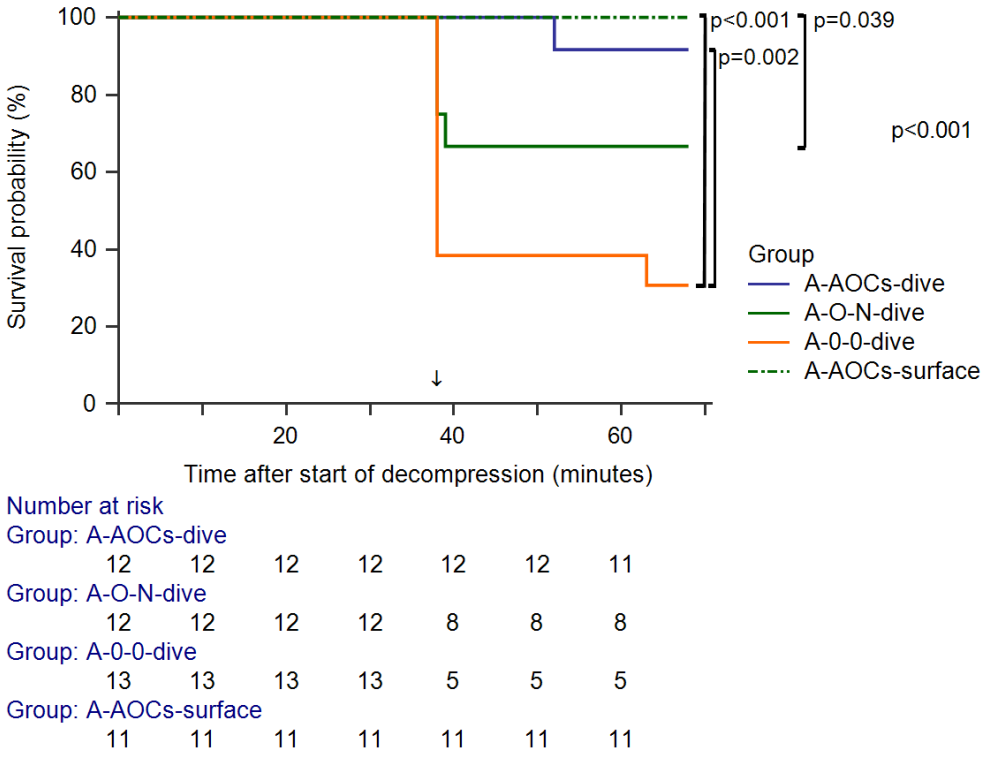

Figure 16. Survival probability.
Results of logrank test. No significant differences between A-AOCs-dive and A-O-N-dive (p=0.122), A-AOCs-dive and A-AOCs-surface (p=0.338), and A-O-N-dive and A-0-0-dive (p=0.078).
↓ indicates the timepoint of opening the compression chamber.

4.3. **Results of autopsy**

Autopsy was performed in all animals with special regard to signs of decompression associated organ damage. A-0-0-dive animals showed a significantly higher occurrence of foamy blood in the right heart and in the portal and/or mesenteric veins as compared with A-AOCs-dive animals (**17**). Foamy blood and/or gas bubbles in tissues were found in 4 of 12 animals (33%) of the A-O-N-dive group, in 9 of 13 animals (69%) of the A-0-0-dive group but in none of the animals of the A-AOCs-dive group.

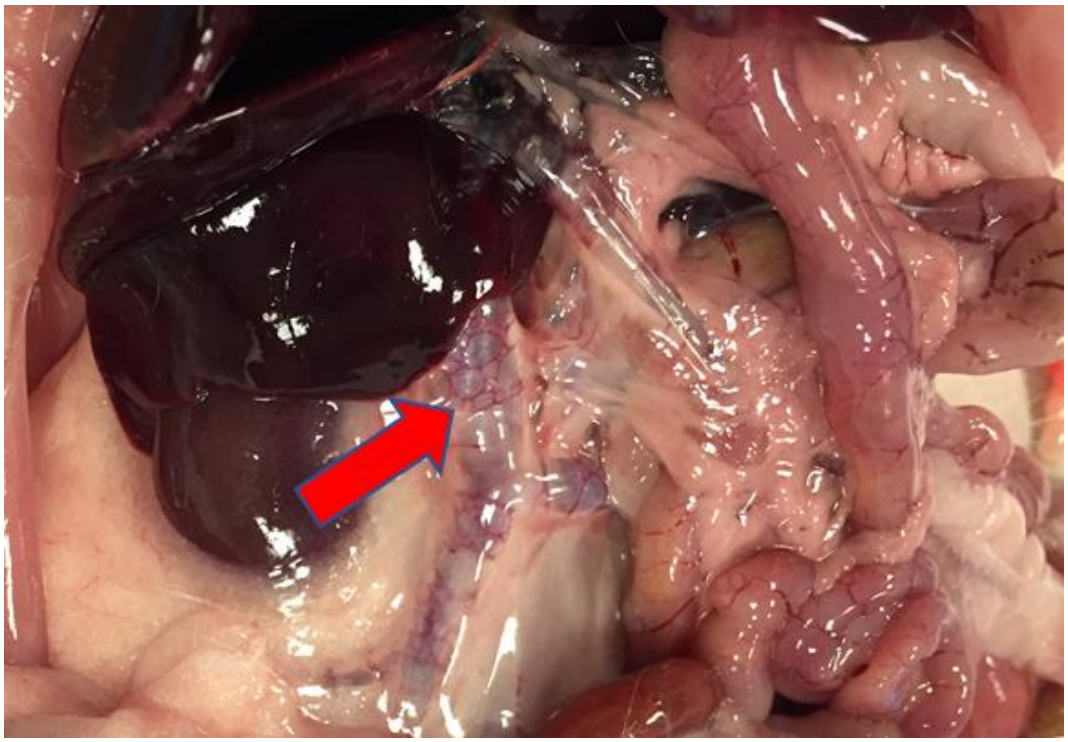

Figure 17. Foamy blood in the portal and mesenteric veins (animal of the control group).

4.4. **Histological assessment**

4.4.1. **Liver**

Pre-dive treatment with A-AOCs was associated with significantly less histological changes in the liver, higher macrophages accumulation and less blood congestion in the spleen compared to A-0-0 treated animals.

A-AOCs-dive animals showed no significant differences of histological gradings for vacuolization (**Figure 18 A-C**), circulatory disorder (**Figure 19 A-C**), hepatocyte damage (**Figure 20 A,B**) and sinusoid congestion (**Figure 21 A-C**) as compared to non-diving A-AOCs-surface animals. In contrast A-O-N-dive- and A-0-0-dive- animals showed a significantly higher grading in all of these parameters than the animals of the A-AOCs-surface group ($p \leq 0.001$). Histological gradings for circulatory disorder (**Figure 19 A-C**), hepatocyte damage (**Figure 20 A,B**) and sinusoid congestion (**Figure 21 A-C**) were significantly different between A-AOCs-dive and A-O-N-dive animals, only the histological grade of vacuolisation (**Figure 18 A-C**) showed no significant differences between these groups ($p = 0.142$). Histological assessment of A-AOCs-dive compared with A-0-0-dive animals revealed significantly less vacuolization ($p<0.001$) (**Figure 18 A-C**), circulatory disorder ($p<0.001$) (**Figure 19 A-C**), hepatocyte damage ($p<0.001$) (**Figure 20**), and sinusoid congestion

(p<0.001) (**Figure 21 A-C**). Examples of histological sections demonstrate the degree of severity of histopathological changes (**Figure 18, 19, 21 B, C**).

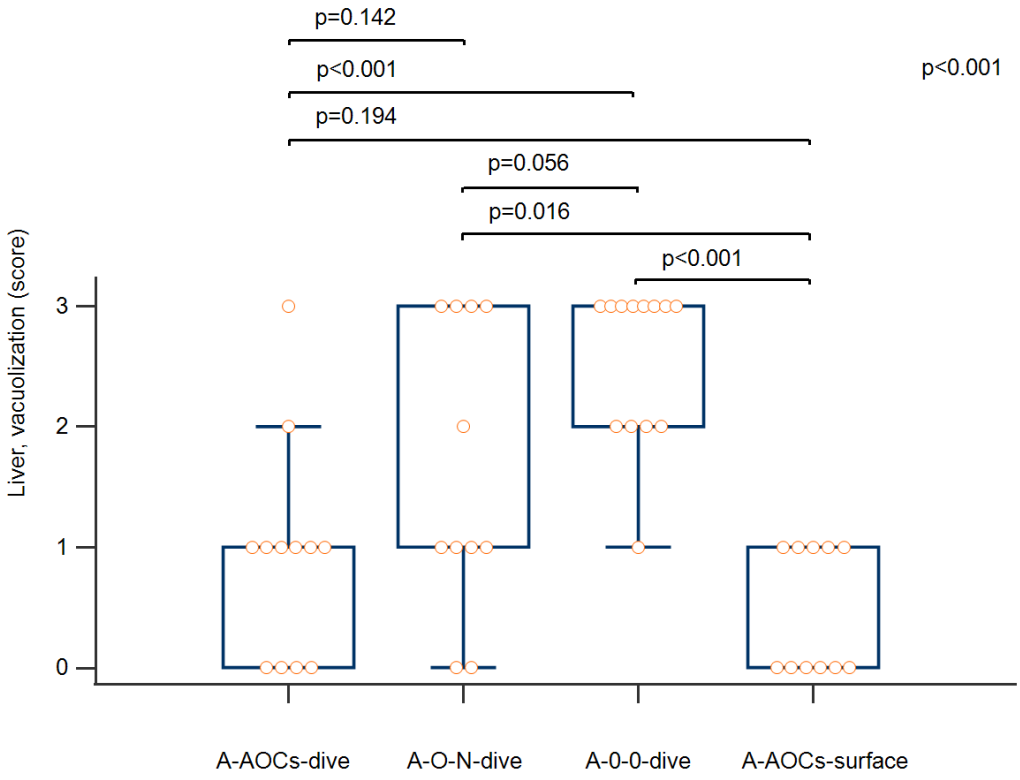

Figure 18 A. Liver, vacuolisation score.
Results of Kruskal-Wallis and Mann-Whitney test.

Histology of the liver: **Figure 18 B,C** show histological specimen as an example for vacuolization grade 0 in an A-AOCs-dive animal (**B**) and grade 3 in an A-O-N-dive animal (**C**).

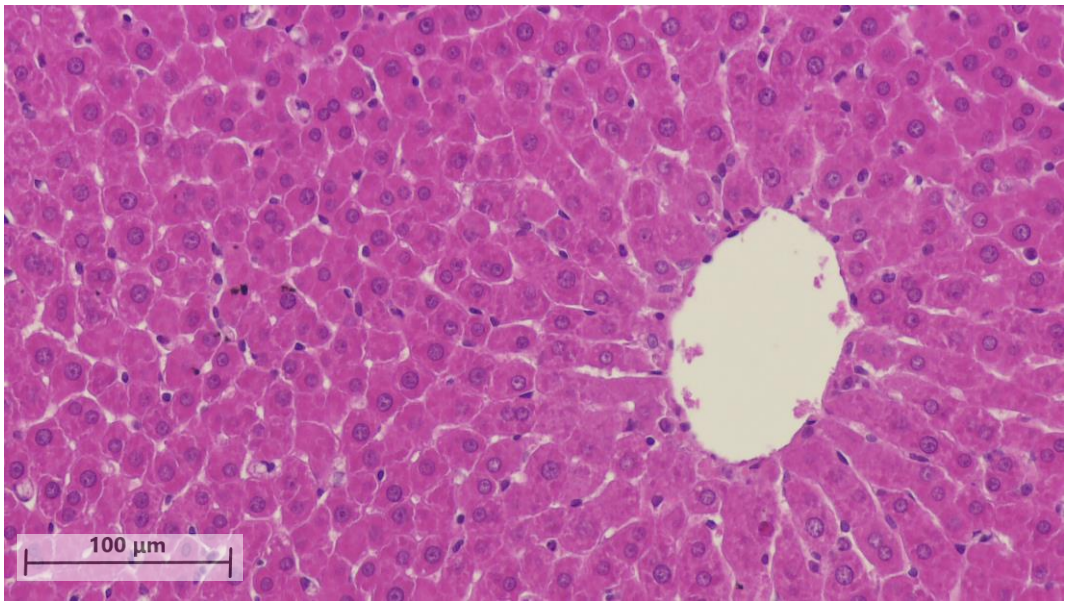

Figure 18 B. Example for histology of the liver, vacuolisation grade 0.

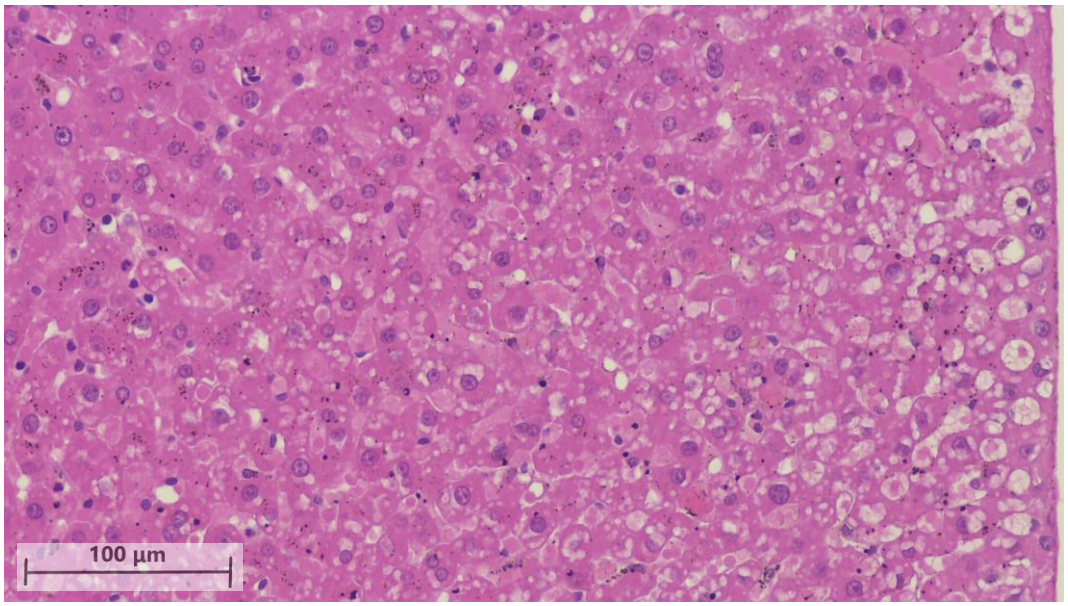

Figure 18 C. Example for histology of the liver, vacuolisation grade 3.

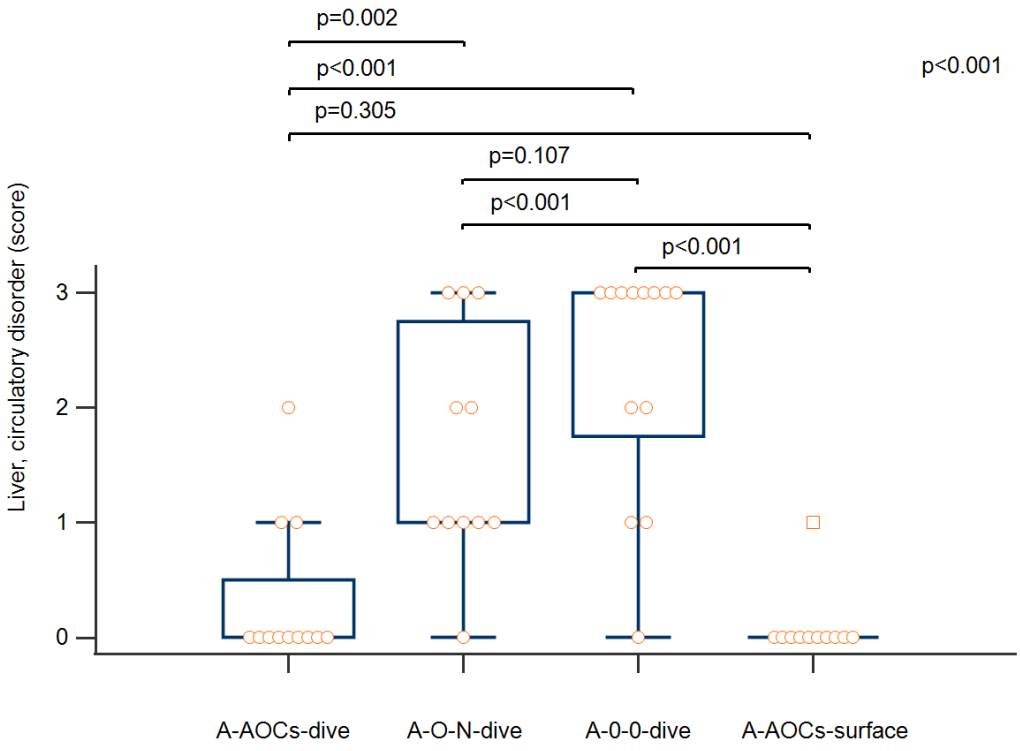

Figure 19 A. Liver, circulatory disorder score.
Results of Kruskal-Wallis and Mann-Whitney test.

Histology of the liver: **Figure 19 B, C** shows histological specimen as an example for circulatory disorder grade 0 in an A-AOCs-dive animal (**B**) and grade 3 in an A-O-N-dive animal (**C**).

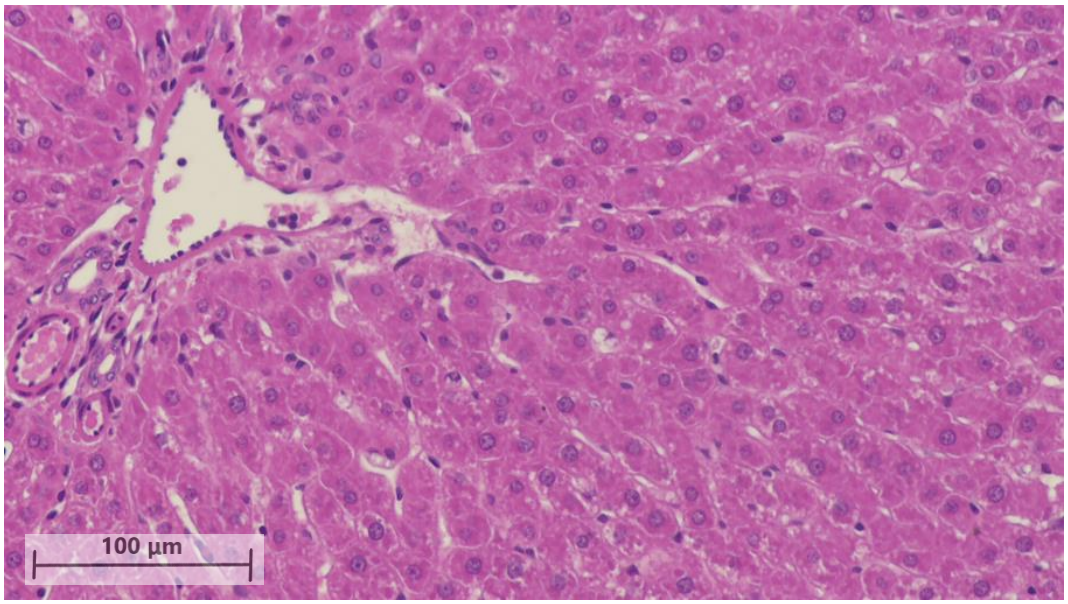

Figure 19 B. Histology of the liver, circulatory disorder grade 0.

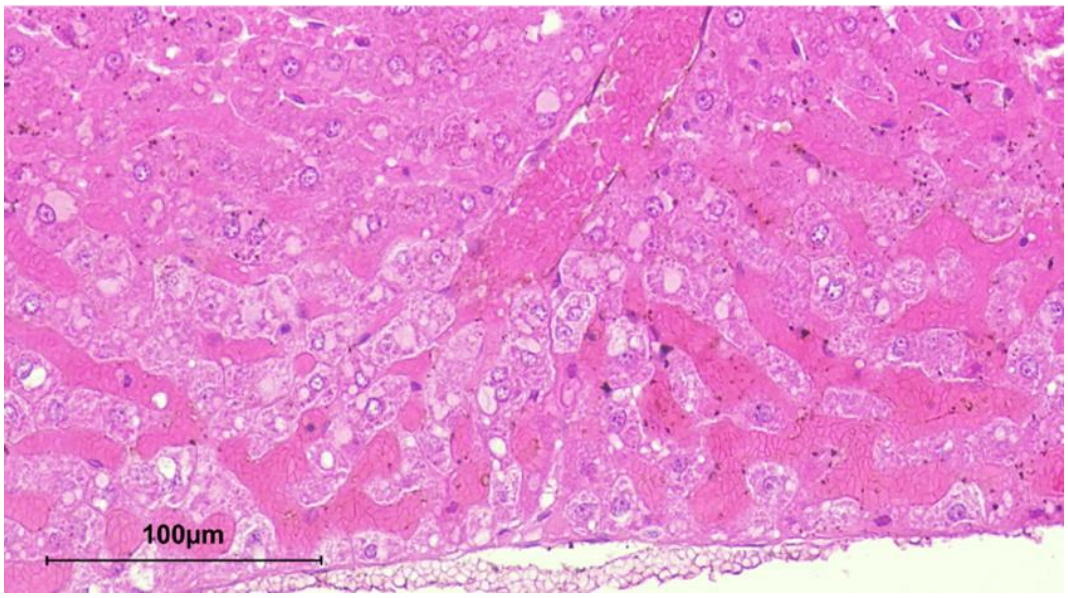

Figure 19 C. Histology of the liver, circulatory disorder grade 3.

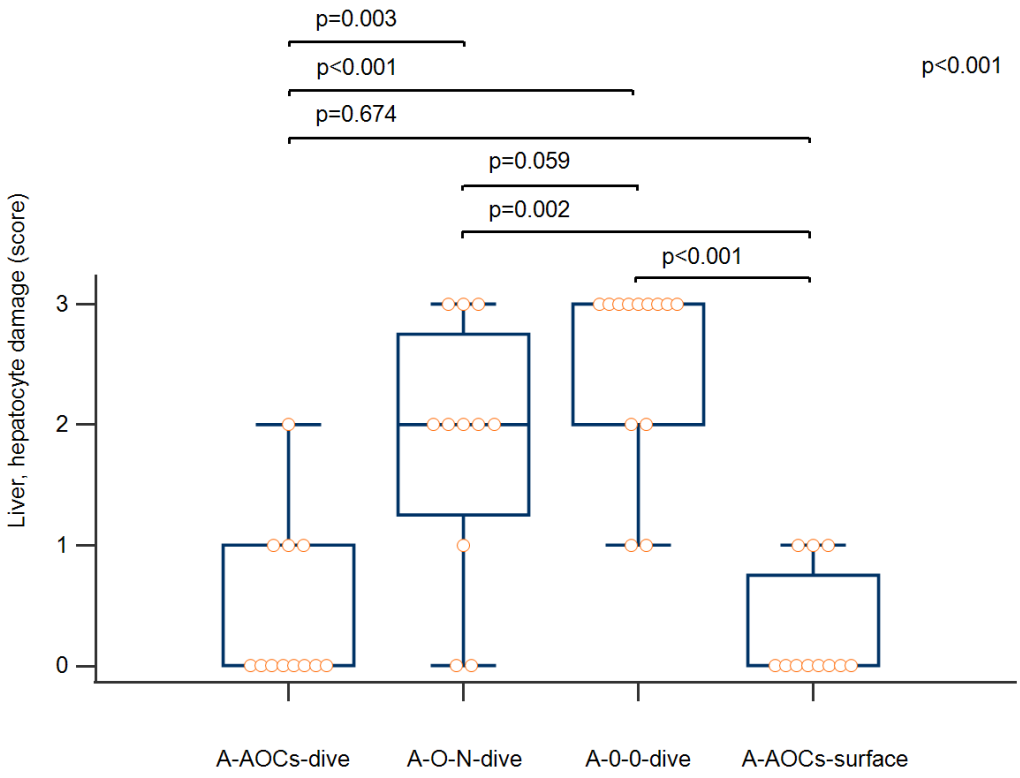

Figure 20. Liver, hepatocyte damage score.
Results of Kruskal-Wallis and Mann-Whitney test.

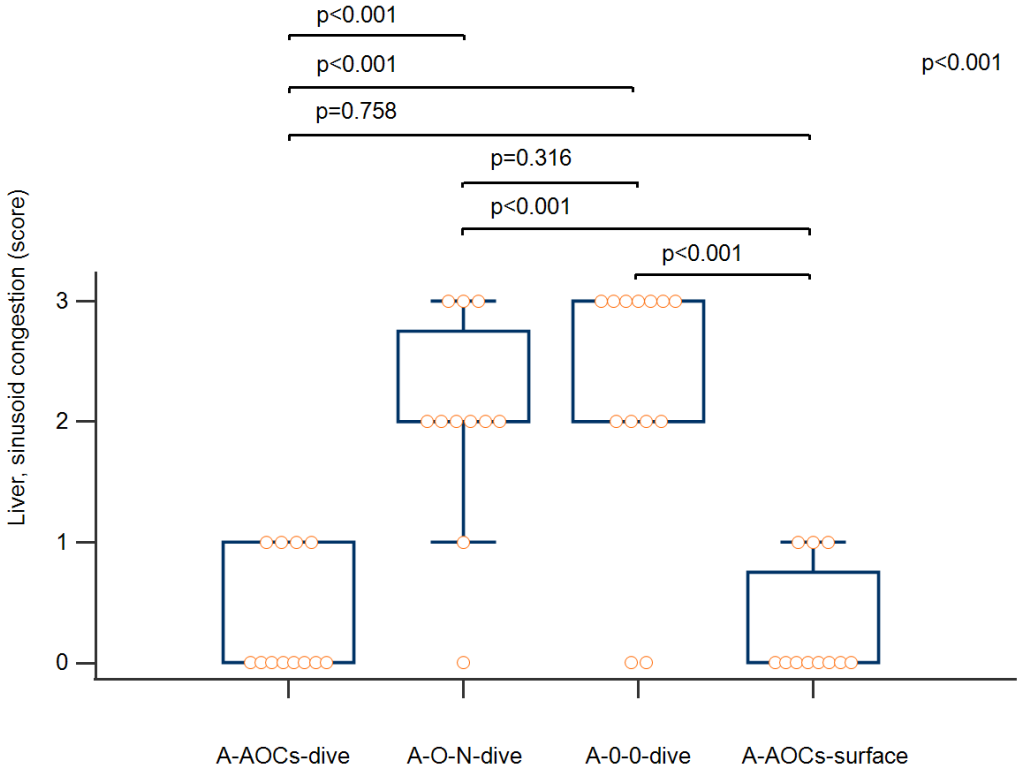

Figure 21 A. Liver, sinusoid congestion score.
Results of Kruskal-Wallis and Mann-Whitney test.

Histology of the liver: **Figure 21 B, C** shows histological specimen as an example for sinusoid congestion grade 0 in an A-AOCs-dive animal (**B**) and grade 3 in an A-O-N-dive animal (**C**).

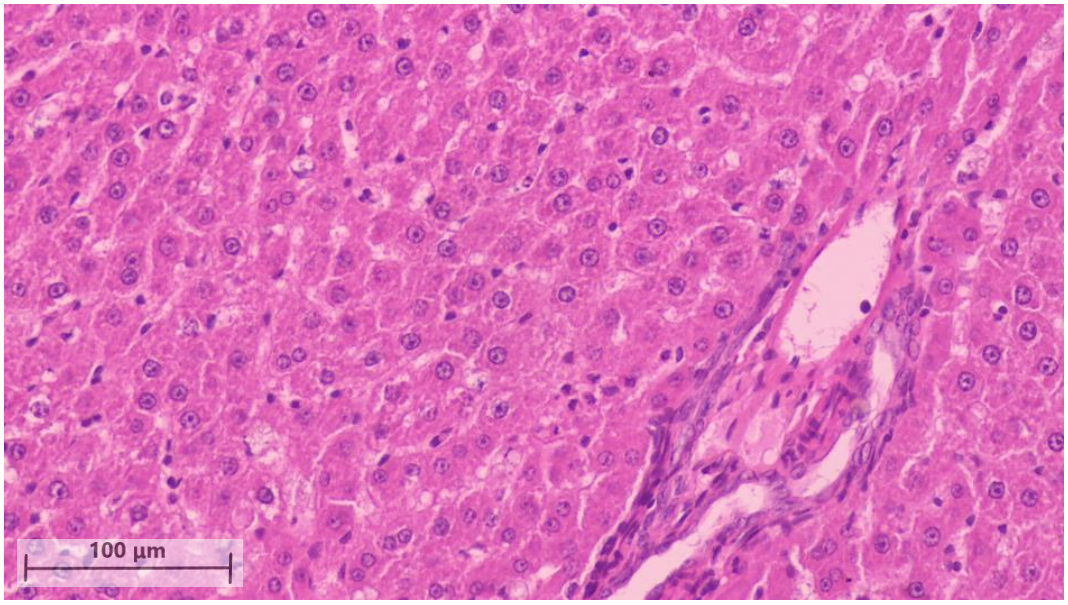

Figure 21 B. Histology of the liver, sinusoid congestion grade 0.

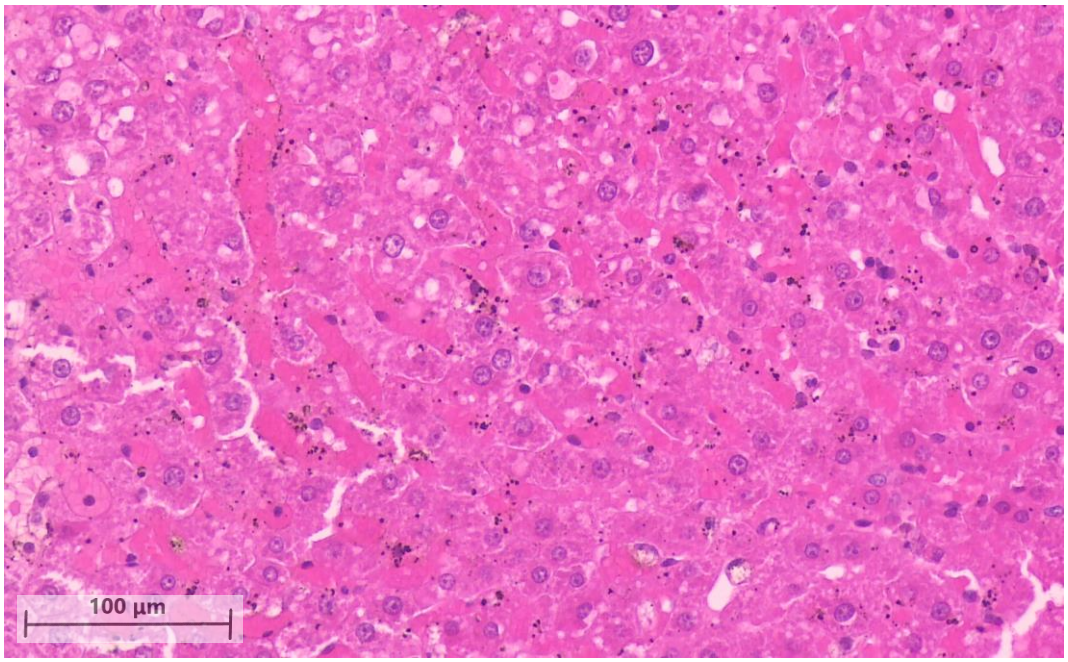

Figure 21 C. Histology of the liver, sinusoid congestion grade 3.

4.4.2. **Kidney**

A-AOCs-dive animals showed no significant difference of histological grading in blood accumulation in the medullo-cortical junction of the kidney compared to non-diving A-AOCs-surface animals. Histological grading of this parameter was significantly higher in A-0-0-dive (p=0.002) and A-O-N-dive animals (p=0.009) than in the A-AOCs-surface group. There was a significantly less pronounced blood accumulation between renal cortex and medulla in A-AOCs-dive animals compared to A-0-0-dive animals (**Figure 22 A-C**).

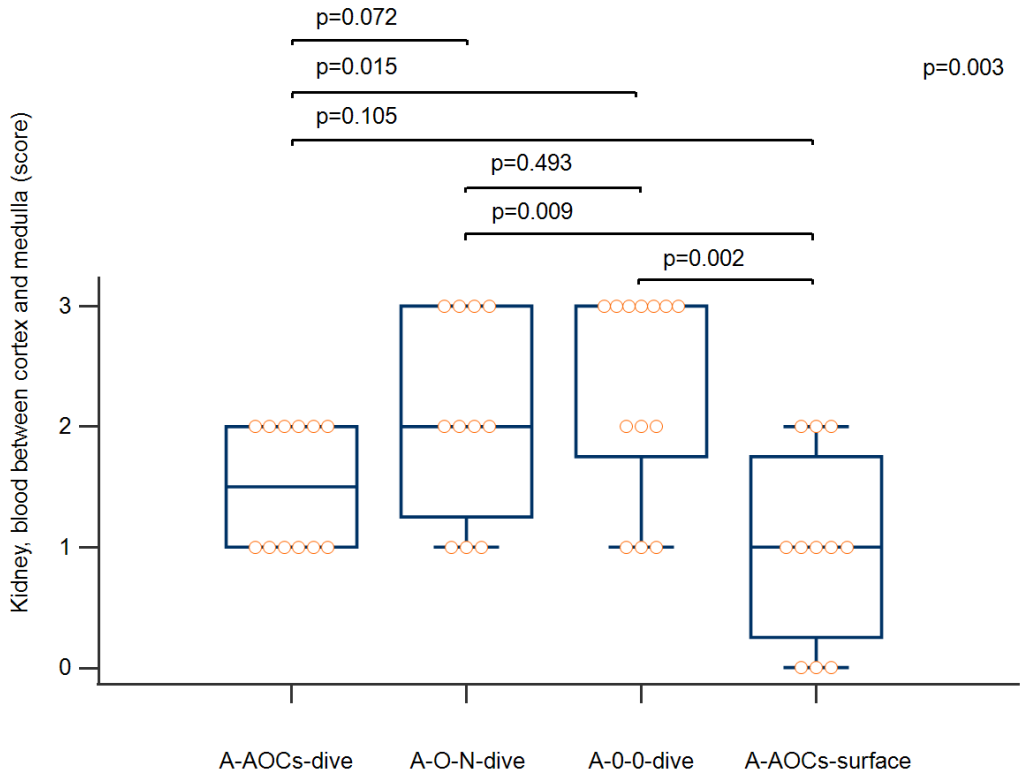

Figure 22 A. Kidney, blood in the medullo-cortical junction score.
Results of Kruskal-Wallis and Mann-Whitney test.

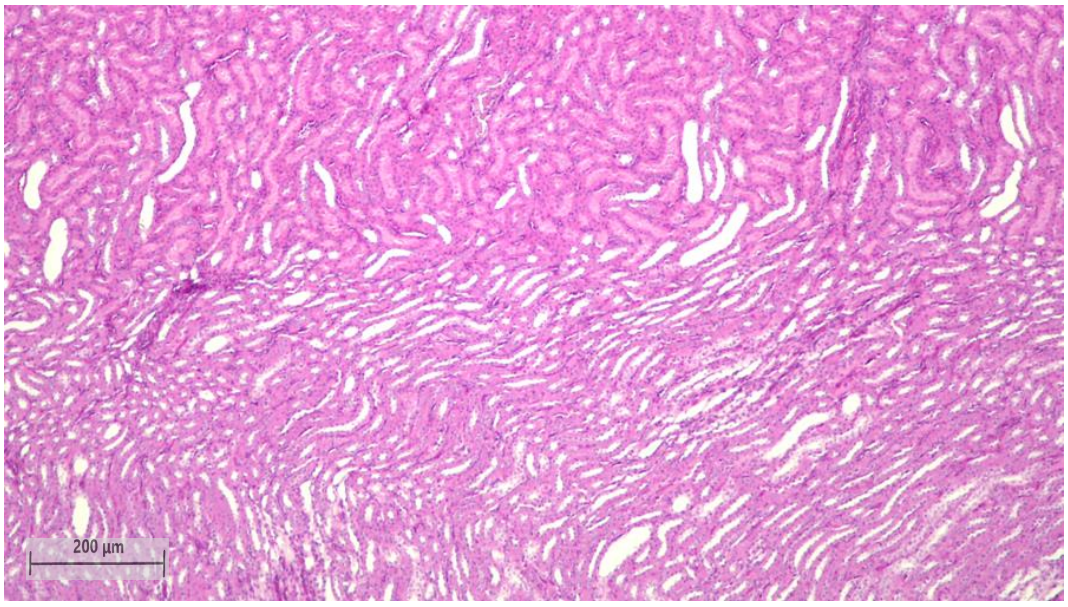

Figure 22 B. Histology kidney, accumulation of blood in the medullo-cortical junction grade 0.

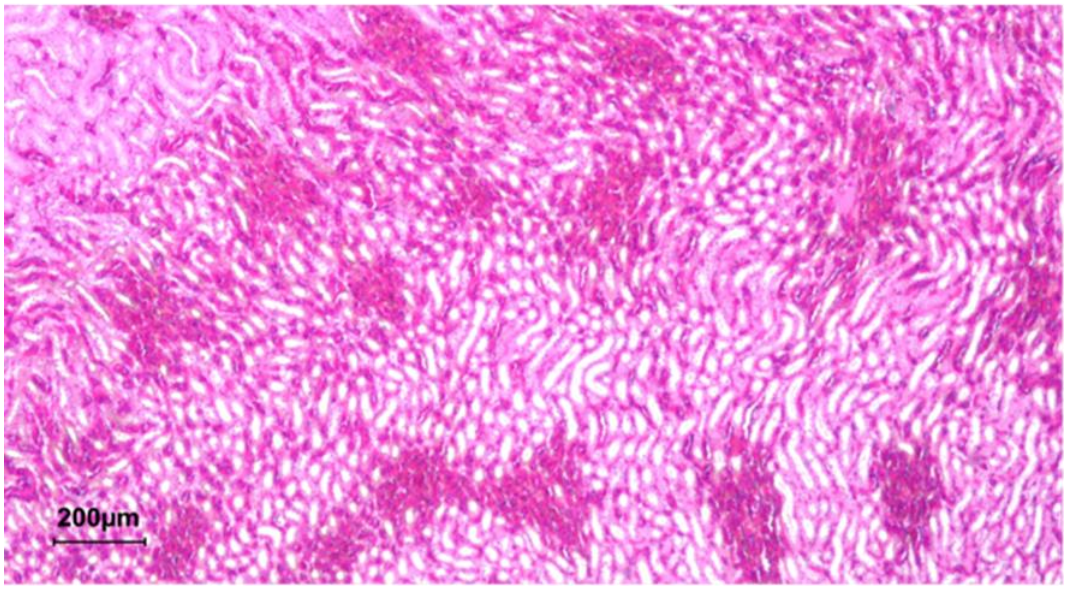

Figure 22 C. Histology kidney, accumulation of blood in the medullo-cortical junction grade 3.

4.4.3. **Spleen**

A-AOCs-dive and A-AOCs-surface animals showed a significant accumulation of macrophages in the spleen compared to A-0-0-dive ($p<0.001$ each) and A-O-N-dive animals ($p \leq 0.001$ each). Accumulation of macrophages is significantly associated with application of A-AOCs (**Figure 23 A**). A significantly lower accumulation of blood ($p<0.001$ each) was verified in A-AOCs-dive compared with A-O-N- and A-0-0-dive animals. There was no significant difference in this parameter between the A-AOCs-dive and the A-AOCs-surface group, whereas A-O-N-dive and A-0-0-dive animals showed significantly higher levels of blood accumulation compared to the A-AOCs-surface group ($p=0.003$ each) (**Figure 24 A**).

Histology specimen show examples of accumulation of macrophages (**Figure 23 B, C**) and blood (**Figure 24 B, C**) in the spleen.

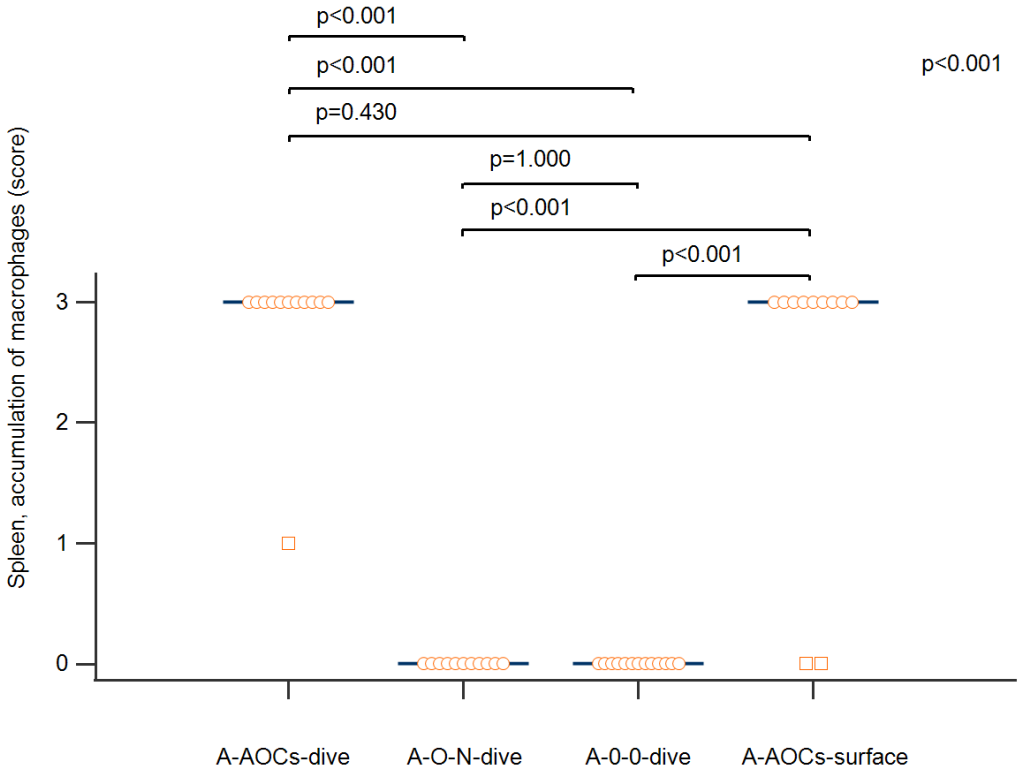

Figure 23 A. Spleen, accumulation of macrophages score.
Results of Kruskal-Wallis and Mann-Whitney test.

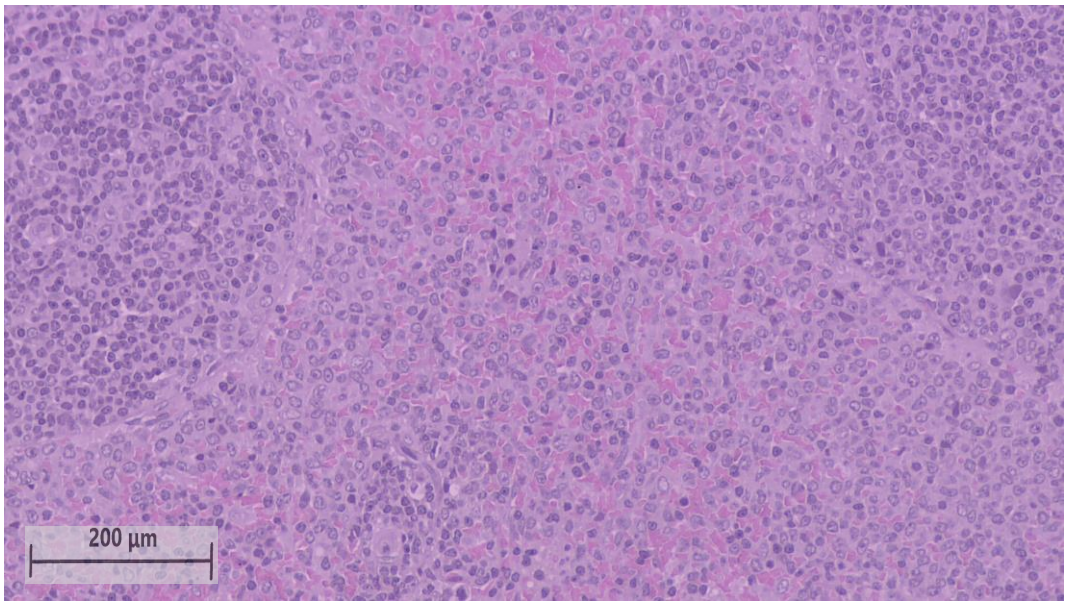

Figure 23 B. Histology, macrophages in the spleen grade 0.

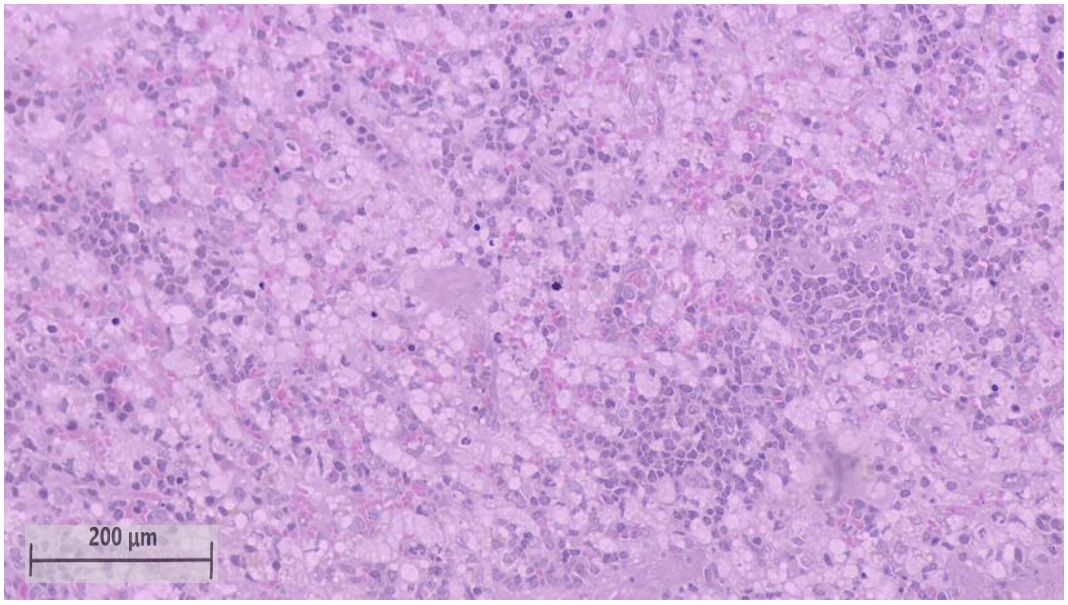

Figure 23 C. Histology, macrophages in the spleen grade 3.

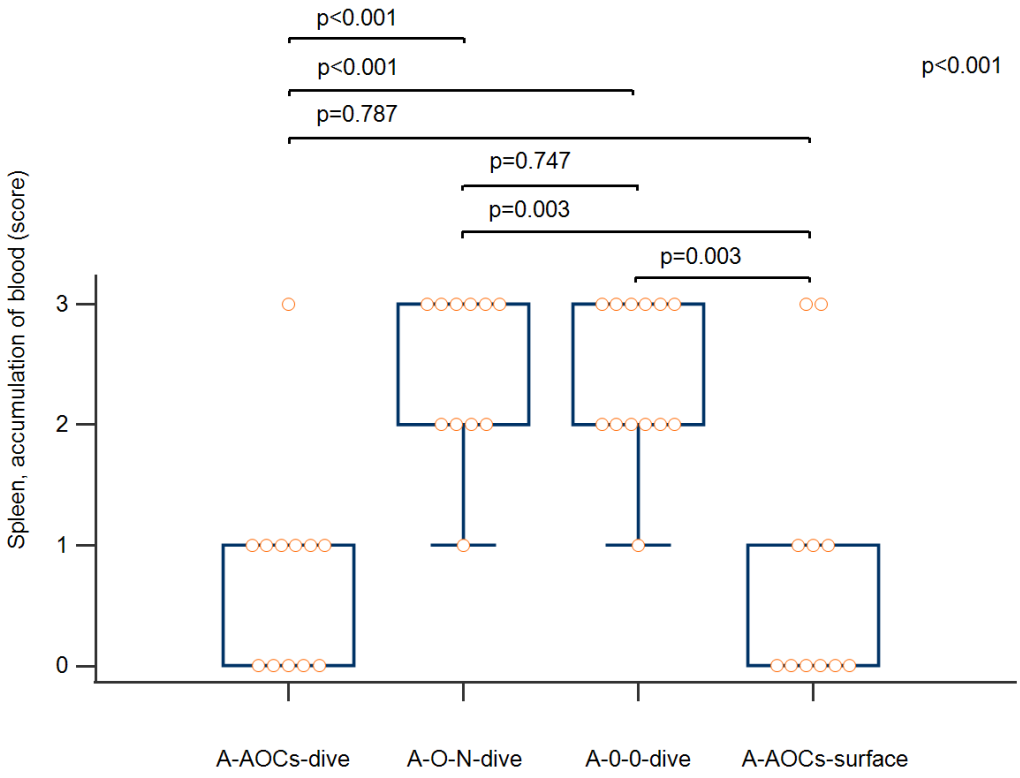

Figure 24 A. Spleen, accumulation of blood score.
Results of Kruskal-Wallis and Mann-Whitney test.

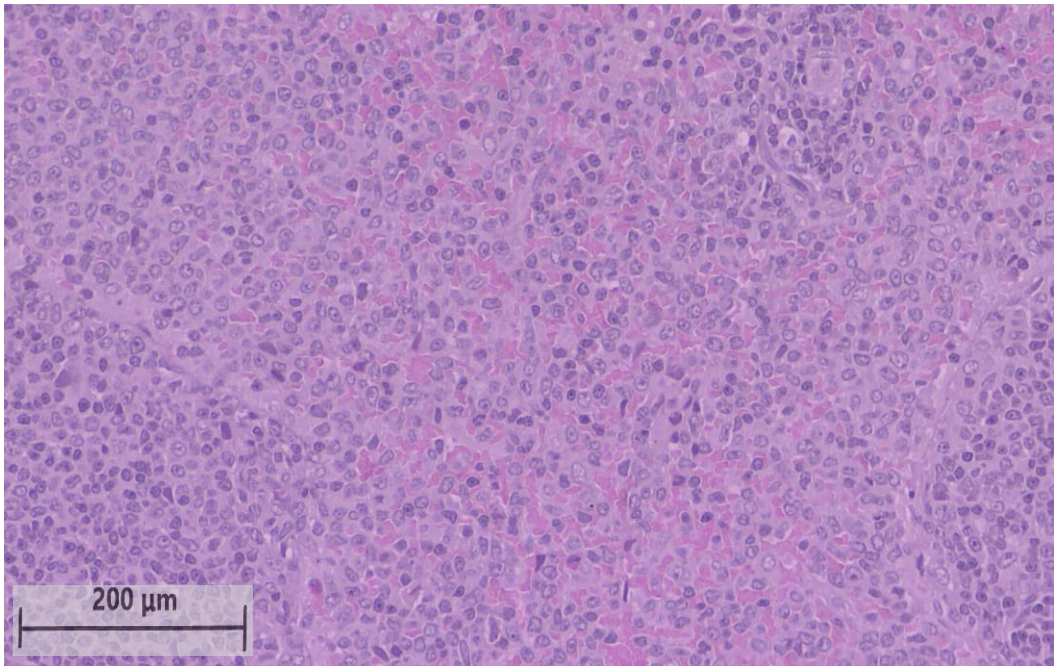

Figure 24 B. Histology of the spleen, accumulation of blood grade 0.

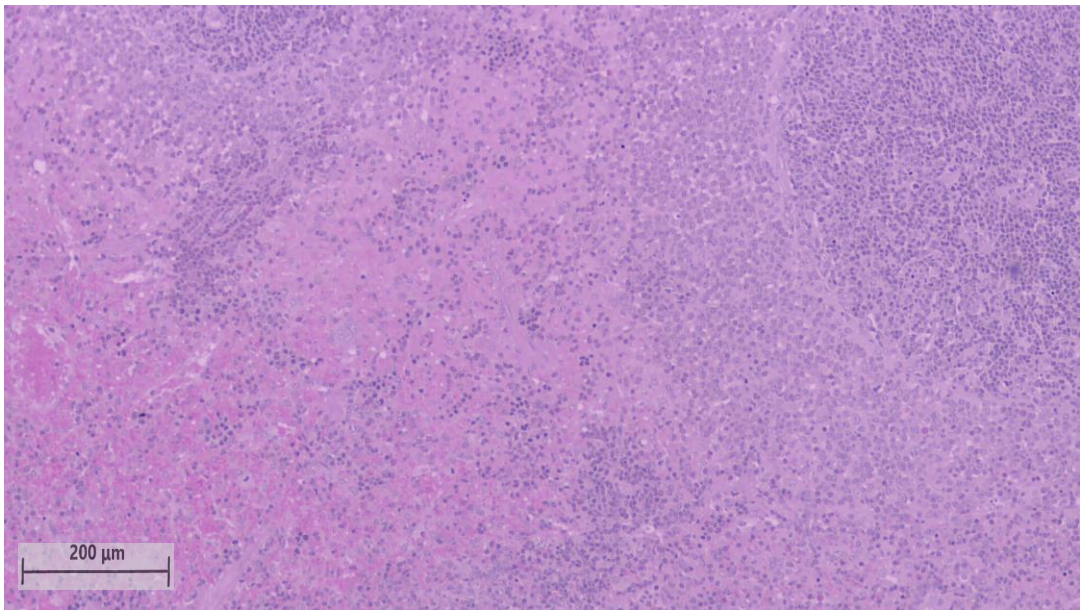

Figure 24 C. Histology of the spleen, accumulation of blood grade 3.

Histological differences were absent between the 4 groups concerning brain, lung, and heart.

4.5. **Plasma parameters**

Subgroup analysis by Dunn's posthoc-test revealed significant differences: compared to non-diving controls (A-AOCs-surface), serum values for lactate ($p=0.007$), and myoglobin ($p<0.001$) showed a significant increase after diving in the A-0-0 group, whereas lactate and myoglobin levels of the A-AOCs-dive and A-O-N-dive group were not significant different from the non-diving group. There was also a significant increase of myoglobin after diving in the A-O-N group ($p=0.005$) and myoglobin was the only serum parameter that was significantly lower in A-AOCs-dive compared to A-0-0-dive animals ($p=0.003$). A-AOCs treated animals didn`t show any significant different values in all tested plasma parameters compared to the A-O-N-dive group and the non-diving animals (A-AOCs-surface group) Urea levels were significantly decreased after diving in the A-O-N ($p=0.005$) and A-0-0 group ($p<0.001$) compared to the A-AOCs surface animals. There was no significant difference between urea values of the A-AOCs-dive group compared to the non-diving group.

The comparison of the plasma parameters ALAT, ASAT, C3c, creatinine, D-dimer, IgM, lactate dehydrogenase and pancreatic amylase failed to offer any significant differences between the three treatment groups and the control animals.

In summary, the quickly responding parameters lactate and myoglobin showed a significant increase in the A-0-0-dive animals whereas this reaction was not detectable in A-AOCs treated animals.

Table 3 gives an overview of all measured post-experimental plasma parameters.

Table 3. Post-experimental plasma parameters.

Plasma parameters	A-AOCs-dive	A-O-N-dive	A-0-0-dive	A-AOCs-surface	p-value[1]
	Median (IQR)				
ALAT [U/l]	96.6 (71.1-112.5)	74.2 (61.7-87.5)	61.9 (59.5-76.0)	89.0 (62.2-142.1)	
ASAT [U/l]	259.5 (190.2-289.5)	157.6 (122.0-239.7)	212.0 (116.7-406.0)	232.7 (166.4-358.0)	
C3c [mg/dl]	25.7 (23.8-27.7)	28.7 (26.6-30.6)	25.8 (22.8-29.1)	26.6 (24.2-28.5)	
CK [U/l]	944.8 (664.5-1426.3)	598.5 (329.0-1319.5)	1102.0 (614.1-2043.3)	678.0 (309.0-829.0)	**p=0.044**
Creatinine [mg/dl]	0.3 (0.3-0.4)	0.3 (0.3-0.4)	0.3 (0.2-0.3)	0.3 (0.3-0.4)	
D-dimer [µg/ml]	0.1 (0.0-0.2)	0.1 (0.0-0.3)	0.1 (0.0-0.2)	0.0 (0.0-0.2)	
IgM [mg/dl]	6.6 (4.3-8.4)	6.6 (3.5-9.8)	6.5 (3.2-7.8)	6.8 (4.6-8.3)	
Lactate [mmol/l]	1.8 (1.6-2.8)	1.4 (1.2-6.9)	8.3 (3.4-9.9)	1.6 (1.4-1.8)	**p=0.048**
p-value[2]			**p=0.007**		
LDH [U/l]	1726.6 (909.3-4346.0)	1704.0 (816.5-4802.3)	1626.5 (1280.8-2918.3)	1106.0 (993.6-2019.0)	
Myoglobin [ng/ml]	9.1 (7.2-17.2)	13.7 (9.1-24.2)	36.9 (13.9-131.7)	7.9 (7.2-9.1)	**p<0.001**
p-value[2]	**p=0.003**				
		p=0.005			
			p<0.001		
P-amylase [U/l]	1597.0 (1432.0-1675.5)	1517.5 (1206.5-1604.5)	1375.5 (1042.0-1443.3)	1606.0 (1393.0-1681.0)	
Urea [mg/dl]	32.2 (28.5-35.9)	30.2 (23.9-34.6)	27.8 (24.5-30.3)	42.5 (33.6-44.9)	**p=0.003**
p-value[2]		**p=0.005**			
			p<0.001		

IQR Interquartile range; [1]Results of Kruskal-Wallis test; [2]Results of Dunn's posthoc-test; p<0.10 listed; p<0.05 in bold.

5. DISCUSSION

In a simulated dive experiment in rats, it could be demonstrated that preventive application of newly developed albumin-derived perfluorocarbon-based artificial oxygen carriers (A-AOCs) shows a positive effect in reducing the occurrence of DCS symptoms because it was associated with a significant higher survival rate and longer survival time compared to the albumin-group (A-0-0) . These findings are consistent with the results of autopsy and histological examination Animals which received A-AOCs intravenously before diving had significantly less DCS associated foaming and organ damage. Pretreatment with albumin-derived neutral oil-based nanocapsules (A-O-N) only led to a slight improvement, and albumin without nanocapsules (A-0-0) was ineffective. DCS induced organ alterations of kidneys, liver and spleen in the A-O-N and A-0-0 control groups can be interpreted as the result of an acute failure of macro- and microcirculation. Functional and pathologic effects of N_2 bubbles in the portal vein circulation of rats after rapid decompression were examined by *L'Abbate et al*. (148). It is presumed that tissue-blood gas exchange in the intestinal wall leads to the formation of bubbles moving to the microvascular system of the liver. Bubble associated embolization results in acute hepatic dysfunction and subsequent liver failure. This DCS induced gas embolism in the liver appears to persist much longer than pulmonary embolism. Our study might give an indication that beside the preventive effect on gas induced embolization in the pulmonary and arterial circulation, A-AOCs could also reduce bubble induced embolism in the liver and portal vein system.

Our present study included a short follow-up of only 30 minutes. It can be argued that the greatest occurrence of bubbles is described 40 to 60 minutes after the dive. This statement is mainly valid, however, for human dives. In rats, it seems that the peak of bubble formation occurs less than 30 minutes post-decompression after an air simulated dive (600 kPa during 60 min followed by a linear decompression at 200 kPa/min) (149). During precursor studies on rats with the „French" hyperbaric protocol, the working group of *François Guerrero* also observed animals up to 2 h post-decompression and found that no signs of DCS appeared later than 15-20 min after decompression. A longer observation time might be useful if the main focus of interest is on the recovery from DCS.

A cardiopulmonary bypass model in rats was used by *Yoshitani et al.* to demonstrate that PFCs effectively reduce the size and quantity of N_2 bubbles (67). This is possible because under normobaric conditions the N_2 transport capacity of PFC reaches nearly 50 volume percent (48). But PFCs not only increase the wash-out and removal of N_2 (65), they also improve the

oxygen delivery to hypoxic tissues (31,150). So, if the hypothesis underlying the use of nanocapsules for the treatment DCS is that they carry more nitrogen and/or oxygen from tissues to lung during and after decompression, it is very likely that they also carry more gases during the dive and, as a result, increase tissues saturation. Nevertheless, if this „loading effect“ during dive is more important than the „unloading effect“ during desaturation, PFD nanocapsules would have increased the DCS ratio. This was not the case in our study. Nevertheless, the lack of increase of the concentration of lactate after administration of nanocapsules (even those without PFD) supports the hypothesis of a lower tissue anoxia and, therefore, increased oxygen transport by nanocapsules.

Beyond the outstanding gas dissolving capacity of PFCs, oils also exhibit increased dissolution of gases. Accordingly, the neutral oil, *Miglyol*®, inside the A-O-N allows the absorption and transport of N_2 to some extent, because N_2 solubility in Miglyol® is four to five times higher than in water (151). Hence, A-O-N may have served as a N_2 carrier with limited transport capability. This could explain why, in our study, A-O-N also exhibit a protective effect on the appearance of DCS, although less marked than A-AOCs and non-statistically significant in regard to A-0-0

Another beneficial function of A-AOCs rests upon their surfactant-like properties. It is well known that small particles have the tendency to adhere to the surface of gas bubbles, hereby reducing the surface tension and leading to stabilization of the resulting dispersion. It can be assumed that nanocapsules such as A-AOCs and A-O-N covering the surface of the N_2 bubbles prevent their adhesion to the endothelium, thus, promoting N_2 transport and wash-out. This so called *Pickering stabilization* (142) could prevent the damaging interaction between N_2 bubbles and the endothelium (comparable to the effect of added emulsifiers in previous preparations), resulting in a reduced platelet-mediated thrombin production (10, 68). In addition, a direct mechanical effect is possible as the comparably dense PFC-filled A-AOC and also, albeit to a much smaller extent, other nanocapsules such as A-O-N are expected to develop an abrasive effect, which by itself could clean the endothelial tissue from adherent bubbles.

Elevations in plasma parameters such as CK, LDH and hepatic transaminase levels have been described in different studies as often associated with AGE and following hepatic injury (152,153). In a study with rats, *Freeman et al.* (1976) found elevated levels of LDH and CK in moderate DCS, whereas AST and ALT elevations were observed only in severe DCS (41). This increase in enzymatic activities was measured one hour after decompression. After 24 hours, with the exception of AST, all enzyme activities had reverted nearly to control level. *Williams et al.* (1988) described an extreme CK elevation in a diver`s accident reaching the peak of 5418

U/L after 3 days (154). Within the constraints of the relatively short observation period of 30 minutes in the present study, exclusively quickly responding plasma parameters such as lactate and myoglobin increased significantly . In comparison with non-diving controls (A-AOCs-surface), lactate and myoglobin values showed a significant DCS-induced increase in the A-0-0 group, but not in the A-AOCs and A-O-N group, respectively. Since tissue hypoperfusion is the most common cause of lactate elevation, this parameter is associated with the degree of circulatory failure. Myoglobin elevation is related to rhabdomyolysis, caused by multiple AGE to the skeletal muscles and liver as in case of severe DCS. The significantly smaller increases of lactate and myoglobin are in accordance with the histological findings of less severe hepatic cell damage in A-AOCs-treated animals .

Since a series of animal studies in different species (hamster, rat, and swine) has demonstrated the potential of intravenously administered PFC preparations (such as *Oxygent*® and *Fluosol-DA*®) as non-recompressive therapeutics of DCS (48, 89, 96, 100, 102), these positive results are hardly surprising. However, formerly used emulsion-based formulations are associated with the considerable handicap of increased retention time and increased side-effects mainly caused by the emulsifier (64, 155). One of the most promising candidates from these DCS animal studies, *Oxygent*®, was also tested in several clinical trials, e.g., in cardiac surgery patients (phase III). Although it had positive effects, it was supposedly associated with severe neurological adverse reactions and its development was stopped in western countries (105). Clinical studies on *Fluosol-DA*® had a similar fate; this perfluorotributylamine preparation obtained temporarily clinical approval for improving oxygenation during coronary angioplasty in USA, Europe, and Japan, but was later withdrawn from the market because of its labor-intensive preparation and severe side-effects (63).

To translate the positive impact of PFCs in DCS treatment to medical practice, novel PFC formulations are urgently needed. All PFC-based products used so far are based on PFC emulsions. However, beside emulsification, encapsulation is another possibility to achieve compatibility of PFCs with the aqueous medium blood. Emulsified PFC preparations, characterized by a mean diameter of 0.4 up to 0.7 µm (85), could lead to an increase of PAP in association with CARPA. The smaller size of the encapsulated A-AOCs (around 80 nm) might be of high importance in order to avoid these adverse reactions (129). A thin capsule wall provides mechanical and dispersive stability while allowing for efficient exchange of respiratory gases (77). Previously employed synthetic polymers for encapsulation led to dangerous immune reactions and therefore proved unsuitable.

Our newly designed A-AOCs combine the non-toxic and non-allergic shell material albumin with a core of perfluorodecalin, a PFC with acceptable organ retention times and less severe side-effects. A-AOCs already proved their functionality as artificial oxygen carrier under in vitro and in vivo conditions (139,140). In the present investigation, the animals of the non-diving control group that received A-AOCs intravenously showed no clinical side-effects during the 112 minutes observation period. There are concerns about oxygen toxicity as a possible cause of convulsions during the follow-up after the simulated dive. If this would be the case, the ratio of rats suffering convulsions after the dive would be the same if the maximal pressure and the dive duration are kept constant. On the contrary, the longer the decompression stops last, the lower is the proportion of rats suffering convulsions after the dive. This is an argument which suggests that convulsions are a sign of DCS affecting the central nervous system.

Histological evaluation revealed a high accumulation of macrophages in the spleen of all animals treated with A-AOCs (irrespective of diving) as an expression of the activated reticuloendothelial system (RES) . It is already known from a previous in vivo evaluation of A-AOCs-biocompatibility that nanoparticles such as A-AOCs accumulate in this filter organ prior to elimination by immune cells (85). As in the past, the present study has shown staining in the spleen for foamy vacuolized macrophages after intravenous infusion of A-AOCs. Earlier investigations had already indicated that this uptake into RES cells is typically reflected by transient vacuolization of macrophages after application of different perfluorocarbon-based emulsions (156). The observed moderate tissue damage of the spleen is associated with the red pulp macrophages scavenging the capsules. Macrophages show phagocytic activity and produce inflammatory cytokines. Polarized macrophage activation seems to be a key component in pathology. Inflammatory cytokines like IFN γ or TNF α, pathogen associated molecular patterns, and damage-associated molecular patterns induce M1-polarized activation, whereas Th2 cytokines like IL-4 or IL-13, anti-inflammatory molecules like IL-10 or AMP, and immunocomplexes induce M2-polarized activation. Epigenetic modifications with involvement of miRNAs, histone methylation and acetylation play a role as regulators of phagocyte activation and function (157). The elimination process observed in the spleen could not be classified as pathophysiological and histological assessment of other organs was normal. In accordance with our previous findings, macro- and microcirculation appear to not be significantly affected by A-AOCs. Plasma parameters did not show any changes in comparison with control animals treated with albumin from earlier biocompatibility studies (85).

There are several limitations of this study. First of all, the number of animals in each study group was small, especially in the control group (n=11). According to sample size calculation at least 12 animals would have been necessary, consequently statistical power is reduced. Initially 15 rats had been provided for each group, but we had to exclude a total of 12 animals from the study because of failed or incomplete injection of the test substance in the tail vein. The procedure of this injection was a technical challenge, but successful application was verified by detection of a white pellet of nanocapsules in the blood sample collected for plasma analysis . If this white pellet was missing, we concluded insufficient application and the animal was excluded from the study. In the ongoing extension study we implemented venous catheters prior to the air dive with a subsequent recovery period of about 2 weeks prior to the simulated dive. In this way the complete application of the test substance can be ensured. Another limitation already mentioned is the relatively short observation period. An extended follow-up would allow more reliable statements about the recovery from DCS. Furthermore, the choice of the diving profile used for these experiments can be discussed. The literature review reveals that different working groups are using diving profiles for rats with a maximum absolute pressure in the range between 500 kPa to 1600 kPa. (51-58). We decided to use the same profile as *de Maistre* 2016 (58) based on the long-term experience of *Francois Guerrero* in the field of diving experiments with rats. Because of the limited number of animals, we had to choose a protocol with clear effect and death is a strong endpoint in this study. After the simulated dive 3 out of 4 rats (A-O-N group) and 8 out of 9 rats (A-0-0 group) were found dead in the chamber without the possibility of clearer description of symptoms or the course of DCS. It can be argued that death during diving is not typical for DCS, and it is an obvious limitation of this study that we had no facility to observe the animals during the dive and immediately after the end of diving. So, the exact time of death is unknown, but autopsy and histological assessment demonstrated typical signs of severe DCS in these animals. Finally, the histological assessment must be viewed critically, because a clear evaluation of the severity of histological changes according to modified *Suzuki's criteria* (146) was difficult to apply in practice. In some borderline cases an accurate determination by an experienced pathologist was difficult. Even considering these limitations and taking into account the consistency of clinical findings, the results of autopsy, histological and serum examinations, the present study still confirms that A-AOCs are effective in preventing DCS and offer a good biocompatibility.

Further research is focusing on the optimization of the A-AOCs shell structure and composition in order to obtain stable products with high gas permeability and lowest toxicity. In collaboration with the working group of *Francois Guerrero*, we started with a therapeutic

study to verify if the post-dive application of PFC-nanocapsules alleviates the symptoms and consequences of DCS in rodents. An additional positive effect could be achieved by oxygen saturation of the A-AOCs in order to reduce the number and size of static metabolic bubbles as shown by *Imbert et al.* (158). In any case, the A-AOCs technology opens up the possibility of taking full advantage of the therapeutic potential of PFCs in the future.

6. CONCLUSIONS

Although the therapeutic potential of perfluorocarbons (PFC) in decompression sickness (DCS) has been known for decades, PFC emulsion-based preparations are not accepted for human use by regulatory authorities mainly because of relevant side-effects and long organ retention time. An alternative way to assemble a stable solution without these disadvantages is the use of PFC nanocapsules with the amphiphilic envelope albumin. Our recently designed Albumin-derived perfluorocarbon-based nanoparticles (A-AOCs), which have been proven to be safe and efficient oxygen carriers for in vivo conditions, are used in a rat model as a preventive measure for DCS. The effects of A-AOCs on the severity of DCS and on the reduction of tissue damage by intravenous application before exposing rats to decompression trauma were demonstrated in an established model. Preventive intravenous application of A-AOCs proved to be well tolerated and effective in reducing the occurrence of DCS. Treated animals showed a significantly higher survival rate, longer survival time and less symptoms compared to the group which received serum albumin only. These positive results were confirmed by analysis of histological examinations and fast reacting plasma parameters.

7. SUMMARY

Effects of newly designed albumin-derived perfluorocarbon-based nanoparticles in the therapy of decompression induced gas embolisms in rats

For three decades, studies have attempted to demonstrate the therapeutic efficacy of perfluorocarbons (PFCs) in reducing the onset of decompression trauma. However, none of these emulsion-based preparations are accepted for therapeutic use in the western world, mainly because of severe side-effects and a long organ retention time. A new development to guarantee a stable dispersion without these disadvantages is the encapsulation of PFCs in nanocapsules with an albumin shell.

Purpose:

Newly designed albumin-derived perfluorocarbon-based artificial oxygen carriers (A-AOCs) are used in a rodent in-vivo model as a preventive therapy for decompression sickness (DCS).

Methods:

Thirty-seven rats were treated with either A-AOCs (n=12), albumin nanocapsules filled with neutral oil (A-O-N, n=12) or 5% human serum albumin solution (A-0-0, n=13) before a simulated dive. Eleven rats, injected with A-AOCs, stayed at normal pressure (A-AOCs-surface). Clinical, laboratory and histological evaluations were performed.

Results:

The occurrence of DCS depended on the treatment group. A-AOCs significantly reduced DCS-appearance and mortality. Furthermore, a significant improvement of survival rate was found (A-AOCs compared with A-0-0). Histological assessment of A-AOCs-dive compared with A-0-0-dive animals revealed significantly higher accumulation of macrophages, but less blood congestion in the spleen and significantly less hepatic circulatory disturbance, vacuolisation, and cell damage. Compared to non-diving controls lactate and myoglobin showed a significant increase in the A-0-0- but not in the A-AOCs-dive group.

Conclusion:

Intravenous application of A-AOCs was well tolerated and effective in reducing the occurrence of DCS, animals showed significantly higher survival rates and less symptoms compared to the albumin group (A-0-0). Analysis of histological results and fast reacting plasma parameters confirmed the preventive properties of A-AOCs.

8. SAŽETAK

Učinci novih perfluorokarbonskih nanočestica stvorenih pomoću albumina u liječenju plinskih embolizama uzrokovanih dekompresijom u štakora.

Istraživanja kojima se ispituje moguća terapijska učinkovitost perfluorokarbona (PFC) u smanjenju dekompresijske traume traju već više od tri desetljeća. Unatoč tome, niti jedan od PFC emulzijskih pripravaka nije odobren u terapijske svrhe u zapadnom svijetu, uglavnom zbog ozbiljnih nuspojava i produljenog zadržavanja u raznim organima. Nova vrsta PFC pripravka, u obliku nanokapsula s albuminskom ovojnicom, bi mogla omogućiti stabilnu smjesu bez ovakvih nedostataka.

Svrha:

Ispitati novu vrstu prenositelja kisika (A-AOC), koji su bazirani na PFC tehnologiji i uključuju albuminsku ovojnicu, kao moguću preventivnu terapiju u štakorskom *in vivo* modelu dekompresijske bolesti (DCS).

Metode:

Trideset sedam štakora je tretirano jednim od sljedećih pripravaka: A-AOC (n=12), albuminskim nanokapsulama ispunjenima neutralnim lipidima (A-O-N, n=12) ili 5 % otopinom albumina ljudskog seruma (A-0-0), a prije simuliranog zarona. Dodatnih jedanaest štakora je primilo A-AOC, ali su potom bili izloženi normalnom tlaku zraka (A-AOC-Površina). Potom je učinjena njihova klinička, laboratorijska i histološka analiza.

Rezultati:

Pojava dekompresijske bolesti je ovisila o vrsti tretmana. U A-AOC štakora je primijećena značajno smanjena incidencija DCS-a i mortaliteta (u usporedbi s A-0-0 štakorima). Histološka procjena A-AOC štakora, u usporedbi s A-0-0 štakorima, je pokazala značajno veće nakupljanje makrofaga, ali i manju kongestiju krvi u slezeni, kao i značajno manje poremećaje u jetrenoj cirkulaciji, stvaranju vakuola i oštećenju stanica. U usporedbi s kontrolnim životinjama (bez zarona), zabilježen je značajan porast laktata i mioglobina u A-0-0 grupi životinja, ali ne i u A-AOC grupi.

Zaključak:

Eksperimentalne životinje su pokazale dobru toleranciju na intravensku primjenu A-AOC, koja se pokazala i učinkovitom u smanjenju pojavnosti DCS-a, povećanju preživljenja i težini simptoma, u usporedbi s grupom životinja tretiranih albuminom (A-0-0). Analize

histoloških rezultata i brzo reagirajućih parametara iz plazme su potvrdile preventivne osobine A-AOC pripravka.

9. CURRICULUM VITAE

Dirk Mayer, MD

Personal Profile:

Chief of Division of the Gastroenterology, Hepatology, and Infectious diseases in the Department of Internal Medicine at Coburg Hospital. The department includes 12 physicians (4 gastroenterologists).

The Section provides diagnostic evaluation, consultation, medical management, and treatment for patients with disorders of the gastrointestinal tract, liver, and pancreas. Services include endoscopic retrograde cholangiopancreatography, endoscopic management of biliary calculi, endoscopic papillotomy and stenting, diagnostic and therapeutic endoscopy, EMR, ESD, esophageal manometry, evaluation of swallowing disorders, GI function laboratory, laser therapy, tumor palliation, liver biopsy and 24 hour esophageal pH monitoring.

Experience:

Participation in the project Medical school Regiomed in cooperation with the University of Split as a trainer for students

Head of the Department for Gastroenterology, Hepatology, and Infectious diseases at Coburg Hospital (February 2014 to present)

Chief physician of the Department for Hematology and Internal Oncology at Coburg Hospital (April 2012 to February 2014)

Chief physician of the Department for Gastroenterology, Hepatology, and Infectious diseases at Coburg Hospital (November 2005 to April 2012)

Senior physician of the Department for Gastroenterology, Hepatology, and Infectious diseases at Coburg Hospital (October 1997 to November 2005)

Senior physician of the Department for Gastroenterology, Hepatology, Diabetology and Internal Oncology at Worms Hospital (October 1996 to October 1997)

Education:

University postgraduate study program Evidence-based medicine, University of Split School of Medicine (ongoing)

Recognition as gastroenterologist (April 1997)

Recognition as specialist for Internal Medicine (December 1995)

Assistant physician, Gastroenterology Department at the University of Ulm (September 1990 to October 1996)
Doctoral thesis at the University of Ulm: Pseudocysts in chronic pancreatitis, Magna cum laude (July 1990)
License to practice medicine (June 1990)
Junior doctor, Gastroenterology Department at the University of Ulm (November 1998 to April 1990)
State examination (October 1988)
Medical studies at the University of Ulm (September 1982 to October 1988)
High school graduation at Max-Planck-Gymnasium Schorndorf (May 1982)

Publications

The main part of the study included in the thesis was published in the original paper:
Mayer D, Guerrero F, Goanvec C, Hetzel L, Linders J, Ljubkovic M, et al. Prevention of Decompression Sickness by Novel Artificial Oxygen Carriers. Med Sci Sports Exerc. 2020;52(10):2127-35 (159).
The following review article offers a thematic overview:
Mayer D, Ferenz KB. Perfluorocarbons for the treatment of decompression illness: how to bridge the gap between theory and practice. Eur J Appl Physiol. 2019;119(11-12):2421-33 (160).
The results of this study have been presented by the first author at three international meetings:
98th Annual Meeting of the German Physiological Society, Ulm 2019, Poster: *Prevention of decompression illness: recently developed albumin-derived perfluorocarbon-based nanocapsules prove effectiveness on a clinical, biochemical, and histological level. Mayer, D., Guerrero, F., Goanvec, C., Kreczy, A., Ljubkovic, M., Mayer, C., Kirsch, M. and Ferenz, K.B.*
Hyperbaric Medicine & the Brain conference, Tel Aviv 2019, oral presentation: *Newly Designed Albumin-Derived Perfluorocarbon-Based Nanocapsules Improve Clinical Symptoms, Mortality and Histological Findings in Decompression Illness. Mayer, D., Guerrero, F., Goanvec, C., Ljubkovic, M., Mayer, C., Kirsch, M. and Ferenz, K.B.*
UHMS Annual Scientific Meeting, Puerto Rico 2019, poster: *Albumin-derived perfluorocarbon-based nanocapsules as an effective preventive therapy of*

decompression illness: well-proven wine in new bottles. Mayer, D., Guerrero, F., Goanvec, C., Ljubkovic, M., Mayer, C., Kirsch, M. and Ferenz, K.B.

Skills:

Language: German (native), English (fluent), French (intermediate)

References:

Professor Dr. med. Markus Ketteler, Department of Internal Medicine and Nephrology at Robert-Bosch-Hospital, Stuttgart

Professor Dr. med. Johannes Brachmann, Head of Medical School Coburg

10. REFERENCES

1. Vann RD, Butler FK, Mitchell SJ, Moon RE. Decompression illness. The Lancet. 2011;377(9760):153-64.
2. Eckenhoff RG, Olstad CS, Carrod G. Human dose-response relationship for decompression and endogenous bubble formation. J Appl Physiol. 1990;69(3):914-8.
3. Tikuisis P. Decompression theory. In: Alf Brubakk TN, editor. Benett and Elliot´s physiology and medicine of diving. Saunders Book Company, Edinburgh, UK, 5th ed., 2003, pp.419-454.
4. Boycott AE, Damant G, Haldane JS. The prevention of compressed-air illness. Epidemiol Infect. 1908;8(3):342-443.
5. Arieli R. Nanobubbles form at active hydrophobic spots on the luminal aspect of blood vessels: consequences for decompression illness in diving and possible implications for autoimmune disease—an overview. Front Physiol. 2017;8:591-602.
6. Blatteau JE, Souraud JB, Gempp E, Boussuges A. Gas nuclei, their origin, and their role in bubble formation. Aviat Space Environ Med. 2006;77(10):1068-76.
7. Vann R, Grimstad J, Nielsen C. Evidence for gas nuclei in decompressed rats. Undersea Biomed Res. 1980;7(2):107-12.
8. Evans A, Walder D. Significance of gas micronuclei in the aetiology of decompression sickness. Nature. 1969;222(5190):251-2.
9. Thom SR, Yang M, Bhopale VM, Milovanova TN, Bogush M, Buerk DG. Intramicroparticle nitrogen dioxide is a bubble nucleation site leading to decompression-induced neutrophil activation and vascular injury. J Appl Physiol. 2012;114(5):550-8.
10. Eckmann DM, Diamond SL. Surfactants attenuate gas embolism-induced thrombin production. Anesthesiology. 2004;100(1):77-84.
11. Brubakk AO, Neuman TS. Bennett and Elliott's physiology and medicine of diving: Saunders Book Company; 2003.
12. Madden LA, Laden G. Gas bubbles may not be the underlying cause of decompression illness–The at-depth endothelial dysfunction hypothesis. Med Hypotheses. 2009;72(4):389-92.
13. Wang Q, Mazur A, Guerrero F, Lambrechts K, Buzzacott P, Belhomme M, Theron M. Antioxidants, endothelial dysfunction, and DCS: in vitro and in vivo study. J Appl Physiol. 2015;119(12):1355-62.
14. Obad A, Valic Z, Palada I, Brubakk AO, Modun D, Dujić Ž. Antioxidant pretreatment and reduced arterial endothelial dysfunction after diving. Aviat Space Environ Med. 2007;78(12):1114-20.
15. Bennett MH, Lehm JP, Mitchell SJ, Wasiak J. Recompression and adjunctive therapy for decompression illness: a systematic review of randomized controlled trials. Anesth Analg. 2010;111(3):757-62.
16. Balestra C, Germonpré P. Correlation between patent foramen ovale, cerebral “lesions” and neuropsychometric testing in experienced sports divers: does diving damage the brain? Front Psychol. 2016;7:696.
17. Sykes O, Clark JE. Patent foramen ovale and scuba diving: a practical guide for physicians on when to refer for screening. Extreme Physiol Med. 2013;2(1):10.
18. Hallenbeck J. Cinephotomicrography of dog spinal vessels during cord-damaging decompression sickness. Neurology. 1976;26(2):190-9.
19. Nossum V, Koteng S, Brubakk AO. Endothelial damage by bubbles in the pulmonary artery of the pig. Undersea Hyperb Med. 1999;26(1):1-8.
20. Mazur A, Lambrechts K, Buzzacott P, Wang Q, Belhomme M, Theron M, Mansourati J, Guerrero F. Influence of decompression sickness on vasomotion of isolated rat vessels. Int J Sports Med. 2014;35(07):551-8.

21. Mazur A, Lambrechts K, Wang Q, Belhomme M, Theron M, Buzzacott P, Guerrero F. Influence of decompression sickness on vasocontraction of isolated rat vessels. J Appl Physiol. 2016;120(7):784-91.
22. Eftedal OS, Lydersen S, Brubakk AO. The relationship between venous gas bubbles and adverse effects of decompression after air dives. Undersea Hyperb Med. 2007;34(2):99-105.
23. Mollerlokken A, Gaustad SE, Havnes MB, Gutvik CR, Hjelde A, Wisloff U, Brubakk AO. Venous gas embolism as a predictive tool for improving CNS decompression safety. Eur J Appl Physiol. 2012;112(2):401-9.
24. Ljubkovic M, Dujic Z, Møllerløkken A, Bakovic D, Obad A, Breskovic T, Brubakk AO. Venous and arterial bubbles at rest after no-decompression air dives. Med Sci Sports Exerc. 2011;43(6):990-5.
25. Germonpré P, Balestra C. Preconditioning to reduce decompression stress in scuba divers. Aerosp Med Hum Perform. 2017;88(2):114-20.
26. Papadopoulou V, Germonpré P, Cosgrove D, Eckersley RJ, Dayton PA, Obeid G, Boutros A, Tang MX, Theunissen S, Balestra C. Variability in circulating gas emboli after a same scuba diving exposure. Eur J Appl Physiol. 2018;118(6):1255-64
27. Randsøe T. Effect of metabolic gases and water vapor, perfluorocarbon emulsions, and nitric oxide on tissue bubbles during decompression sickness (published dissertation). Dan Med J. 2016;63(5):1-28.
28. Network DA. The DAN annual review of recreational SCUBA diving injuries and fatalities based on 1999 data. Durham, NC: Divers Alert Network. 2001;30.
29. Dart TS, Butler W. Towards new paradigms for the treatment of hypobaric decompression sickness. Aviat Space Environ Med. 1998;69(4):403-9.
30. Thalmann E, editor Principles of US Navy recompression treatments for decompression sickness. Treatment of Decompression Illness, Proceedings of the Forty-fifth Workshop of the Undersea and Hyperbaric Medical Society UHMS, Kensington MD; 1996.
31. Spiess BD. The potential role of perfluorocarbon emulsions in decompression illness. Diving Hyperb Med. 2010;40(1):28-33.
32. Mitchell SJ, Bennett MH, Bryson P, Butler FK, Doolette DJ, Holm JR, Kot J, Lafère P. Pre-hospital management of decompression illness: expert review of key principles and controversies. Diving Hyperb Med. 2018;48(1):45.
33. Ball R, Lehner CE, Parker EC. Predicting risk of decompression sickness in humans from outcomes in sheep. J Appl Physiol. 1999;86(6):1920-9.
34. Boussuges A. A rat model to study decompression sickness after a trimix dive. J Appl Physiol. 2007;102(4):1301-2.
35. Suckow MA, Weisbroth SH, Franklin CL. The laboratory rat: Elsevier; 2005.
36. Bondi M, Cavaggioni A, Michieli P, Schiavon M, Travain G. Delayed effect of nitric oxide synthase inhibition on the survival of rats after acute decompression. Undersea Hyperb Med. 2005;32(2):121-8.
37. Bigley NJ, Perymon H, Bowman GC, Hull BE, Stills Jr HF, Henderson RA. Inflammatory cytokines and cell adhesion molecules in a rat model of decompression sickness. J Interferon Cytokine Res. 2008;28(2):55-63.
38. Lillo R, Parker E. Mixed-gas model for predicting decompression sickness in rats. J Appl Physiol. 2000;89(6):2107-16.
39. Bondi M, Cavaggioni A, Gasperetti A, Rubini A. A new method of measure of bubble gas volume shows that interleukin-6 injected into rats has no effect on gas embolism. Undersea Hyperb Med. 2009;36(2):103.
40. L'Abbate A, Kusmic C, Matteucci M, Pelosi G, Navari A, Pagliazzo A, Longobardi P, Bedini R. Gas embolization of the liver in a rat model of rapid decompression. American

Journal of Physiology-Regulatory, Integrative and Comparative Physiology. 2010;299(2):R673-R82.
41. Freeman DJ, Philp RB. Changes in blood enzyme activity and hematology of rats with decompression sickness. Aviat Space Environ Med. 1976;47(9):945-9.
42. Arieli R, Boaron E, Abramovich A. Combined effect of denucleation and denitrogenation on the risk of decompression sickness in rats. J Appl Physiol. 2009;106(4):1453-8.
43. Bennett P, Hayward A. Relative decompression sickness hazards in rats of neon and other inert gases. Aerosp Med. 1968;39(3):301-2.
44. Blatteau J-E, Brubakk AO, Gempp E, Castagna O, Risso J-J, Vallée N. Sidenafil pre-treatment promotes decompression sickness in rats. PLoS One. 2013;8(4):e60639.
45. Butler BD, Little TM, Sothern RB, Smolensky MH. Circadian study of decompression sickness symptoms and response-associated variables in rats. Chronobiol Int. 2010;27(1):138-60.
46. Arieli R, Svidovsky P, Abramovich A. Decompression sickness in the rat following a dive on trimix: recompression therapy with oxygen vs. heliox and oxygen. J Appl Physiol. 2007;102(4):1324-8.
47. Eftedal I, Jørgensen A, Røsbjørgen R, Flatberg A, Brubakk AO. Early genetic responses in rat vascular tissue after simulated diving. Physiol Genomics. 2012;44(24):1201-7.
48. Spiess B, McCarthy R, Tuman K, Woronowicz A, Tool K, Ivankovich A. Treatment of decompression sickness with a perfluorocarbon emulsion (FC-43). Undersea Biomed Res. 1988;15(1):31-7.
49. Vann R, Thalmann E. Decompression physiology and practice. The Physiology and Medicine of Diving. Bennett PB, Elliott DH. 1993.
50. Dujić Z, Palada I, Obad A, Duplancić D, Baković D, Valic Z. Exercise during a 3-min decompression stop reduces postdive venous gas bubbles. Med Sci Sports Exerc. 2005;37(8):1319-23.
51. Tang S-E, Liao W-I, Wu S-Y, Pao H-P, Huang K-L, Chu S-J. The Blockade of Store-Operated Calcium Channels Improves Decompression Sickness in Rats. Front Physiol. 2020;10(1616).
52. Zhang R, Yu Y, Manaenko A, Bi H, Zhang N, Zhang L, Zhang T, Ye Z, Sun X. Effect of helium preconditioning on neurological decompression sickness in rats. J Appl Physiol. 2019;126(4):934-40.
53. Zhang K, Jiang Z, Ning X, Yu X, Xu J, Buzzacott P, Xu W. Endothelia-Targeting Protection by Escin in Decompression Sickness Rats. Sci Rep. 2017;7(1):41288.
54. Cosnard C, De Maistre S, Abraini JH, Chazalviel L, Blatteau J-E, Risso J-J, Vallée N. Thirty-five Day Fluoxetine Treatment Limits Sensory-Motor Deficit and Biochemical Disorders in a Rat Model of Decompression Sickness. Front Physiol. 2017;8(604).
55. Bao X-C, Chen H, Fang Y-Q, Yuan H-R, You P, Ma J, Wang F-F. Clopidogrel reduces the inflammatory response of lung in a rat model of decompression sickness. Respir Physiol Neurobiol. 2015;211:9-16.
56. Sheppard RL, Regis DP, Mahon RT. Dodecafluoropentane (DDFPe) and Decompression Sickness-Related Mortality in Rats. Aerosp med hum perform. 2015;86(1):21-6.
57. Randsoe T, Meehan CF, Broholm H, Hyldegaard O. Effect of nitric oxide on spinal evoked potentials and survival rate in rats with decompression sickness. J Appl Physiol. 2015;118(1):20-8.
58. de Maistre S, Vallée N, Gempp E, Lambrechts K, Louge P, Duchamp C, Blatteau J-E. Colonic Fermentation Promotes Decompression sickness in Rats. Sci Rep. 2016;6(1):20379.

59. Mazur A, Lambrechts K, Buzzacott P, Wang Q, Belhomme M, Theron M, Mansourati J, Guerrero F. Influence of decompression sickness on vasomotion of isolated rat vessels. Int J Sports Med. 2014;35(7):551-8.
60. Clark LC, Gollan F. Survival of mammals breathing organic liquids equilibrated with oxygen at atmospheric pressure. Science. 1966;152(3730):1755-6.
61. Jägers J, Wrobeln A, Ferenz KB. Perfluorocarbon-based oxygen carriers: from physics to physiology. Pflugers Arch. 2020:1-12.
62. Wesseler EP, Iltis R, Clark Jr LC. The solubility of oxygen in highly fluorinated liquids. J Fluor Chem. 1977;9(2):137-46.
63. Lowe KC. Blood substitutes: from chemistry to clinic. J Mater Chem. 2006;16(43):4189-96.
64. Riess JG. Oxygen carriers ("blood substitutes") raison d'être, chemistry, and some physiology blut ist ein ganz besondrer saft. Chem Rev. 2001;101(9):2797-920.
65. Zhu J, Hullett J, Somera L, Barbee R. Intravenous perfluorocarbon emulsion increases nitrogen washout after venous gas emboli in rabbits. Undersea Hyperb Med. 2007;34(1):7.
66. Spiess BD. Perfluorocarbon emulsions as a promising technology: a review of tissue and vascular gas dynamics. J Appl Physiol (1985). 2009;106(4):1444-52.
67. Yoshitani K, De Lange F, Ma Q, Grocott HP, Mackensen GB. Reduction in air bubble size using perfluorocarbons during cardiopulmonary bypass in the rat. Anesth Analg. 2006;103(5):1089-93.
68. Suzuki A, Armstead SC, Eckmann DM. Surfactant reduction in embolism bubble adhesion and endothelial damage. Anesthesiology. 2004;101(1):97-103.
69. Lanaro R, De Capitani EM, Costa JL, Bucaretchi F, Togni L, Linden R, Barbosa F, Tessaro EP, Bataglion GA, Eberlin MN. Sudden deaths due to accidental intravenous injection of perfluorocarbon during MRI cranial examinations. Forensic Toxicol. 2014;32(2):323-30.
70. Lowe KC. Engineering blood: synthetic substitutes from fluorinated compounds. Tissue Eng. 2003;9(3):389-99.
71. Johnson JL, Dolezal MC, Kerschen A, Matsunaga TO, Unger EC. In vitro comparison of dodecafluoropentane (DDFP), perfluorodecalin (PFD), and perfluoroctylbromide (PFOB) in the facilitation of oxygen exchange. Artif Cell Blood Sub. 2009;37(4):156-62.
72. Riess JG. Understanding the fundamentals of perfluorocarbons and perfluorocarbon emulsions relevant to in vivo oxygen delivery. Artif cell blood sub. 2005;33(1):47-63.
73. Kuznetsova I. Perfluorocarbon emulsions: stability in vitro and in vivo (a review). Pharm Chem J. 2003;37(8):415-20.
74. Basile A, Annesini MC, Piemonte V, Charcosset C. Current Trends and Future Developments on (Bio-) Membranes: Membrane Applications in Artificial Organs and Tissue enineering, Section 12, 191-214. In: Ferenz KB, editor. Artificial Oxygen Carriers: Elsevier; 2018. p. 191-214.
75. Ferenz KB, Waack IN, Mayer C, de Groot H, Kirsch M. Long-circulating poly (ethylene glycol)-coated poly (lactid-co-glycolid) microcapsules as potential carriers for intravenously administered drugs. J Microencapsul. 2013;30(7):632-42.
76. Ferenz KB, Waack IN, Laudien J, Mayer C, Broecker-Preuss M, Groot H, Kirsch M. Safety of poly (ethylene glycol)-coated perfluorodecalin-filled poly (lactide-co-glycolide) microcapsules following intravenous administration of high amounts in rats. Results Pharma Sci. 2014;4:8-18.
77. Stephan C, Schlawne C, Grass S, Waack IN, Ferenz KB, Bachmann M, Barnert S, Schubert R, Bastmeyer M, de Groot H. Artificial oxygen carriers based on perfluorodecalin-filled poly (n-butyl-cyanoacrylate) nanocapsules. J Microencapsul. 2014;31(3):284-92.
78. Laudien J, Groß-Heitfeld C, Mayer C, Groot Hd, Kirsch M, Ferenz KB. Perfluorodecalin-Filled Poly(n-butyl-cyanoacrylate) Nanocapsules as Potential Artificial

Oxygen Carriers: Preclinical Safety and Biocompatibility. J Nanosci Nanotechnol. 2015;15(8):5637-48.
79. Singh R, Nalwa HS. Medical applications of nanoparticles in biological imaging, cell labeling, antimicrobial agents, and anticancer nanodrugs. J Biomed Nanotechnol. 2011;7(4):489-503.
80. Jiang L, Sun H, Yuan A, Zhang K, Li D, Li C, Shi C, Li X, Gao K, Zheng C. Enhancement of osteoinduction by continual simvastatin release from poly (lactic-co-glycolic acid)-hydroxyapatite-simvastatin nano-fibrous scaffold. J Biomed Nanotechnol. 2013;9(11):1921-8.
81. Huang S, Chen G, Chaker M, Ozaki T, Tijssen P, Ma D. Fluorescent-magnetic multifunctional nanoparticles for imaging and drug delivery. Rev Nanosci Nanotechnol. 2013;2(5):346-64.
82. Byagari K, Shanavas A, Rengan A, Kundu G, Srivastava R. Biocompatible amphiphilic pentablock copolymeric nanoparticles for anti-cancer drug delivery. J Biomed Nanotechnol. 2014;10(1):109-19.
83. Xiong Y, Liu ZZ, Georgieva R, Smuda K, Steffen A, Sendeski M, Voigt A, Patzak A, Bäumler H. Nonvasoconstrictive hemoglobin particles as oxygen carriers. ACS nano. 2013;7(9):7454-61.
84. Patil GV. Biopolymer albumin for diagnosis and in drug delivery. Drug Dev Res. 2003;58(3):219-47.
85. Wrobeln A, Laudien J, Gross-Heitfeld C, Linders J, Mayer C, Wilde B, Knoll T, Naglav D, Kirsch M, Ferenz KB. Albumin-derived perfluorocarbon-based artificial oxygen carriers: A physico-chemical characterization and first in vivo evaluation of biocompatibility. Eur J Pharm Biopharm. 2017;115:52-64.
86. Castro CI, Briceno JC. Perfluorocarbon-based oxygen carriers: review of products and trials. Artif Organs. 2010;34(8):622-34.
87. Mattrey RF, Hilpert PL, Long CD, Long DM, Mitten RM, Peterson T. Hemodynamic effects of intravenous lecithin-based perfluorocarbon emulsions in dogs. Crit Care Med. 1989;17(7):652-6.
88. Ingram DA, Forman MB, Murray JJ. Activation of complement by Fluosol attributable to the pluronic detergent micelle structure. J Cardiovasc Pharmacol. 1993;22(3):456-61.
89. Lutz J, Herrmann G. Perfluorochemicals as a treatment of decompression sickness in rats. Pflugers Arch. 1984;401(2):174-7.
90. Vercellotti GM, Hammerschmidt DE, Craddock PR, Jacob HS. Activation of plasma complement by perfluorocarbon artificial blood: probable mechanism of adverse pulmonary reactions in treated patients and rationale for corticosteroids prophylaxis. Blood. 1982;59(6):1299-304.
91. Lane TA. Perfluorochemical-based artificial oxygen carrying red cell substitutes. Transfus Sci. 1995;16(1):19-31.
92. Young LH, Jaffe CC, Revkin JH, McNulty PH, Cleman M. Metabolic and functional effects of perfluorocarbon distal perfusion during coronary angioplasty. Am J Cardiol. 1990;65(15):986-90.
93. Spiess BD, McCarthy R, Piotrowski D, Ivankovich AD. Protection from venous air embolism with fluorocarbon emulsion FC-43. J Surg Res. 1986;41(4):439-44.
94. Ochikubo H, Wada S, Sugawara Y, Sueda T, Matsuura Y. Effect of FC43se on Endotoxin-induced Disseminated Intravascular Coagulation in Rats. Hiroshima J Med Sci. 1999;48:71-7.
95. Bito A, Inoue K, Asano M, Ando S, Takaba T. Experimental myocardial preservation study of adding perfluorochemicals (FC43) in lidocaine cardioplegia. Ann Thorac Cardiovasc Surg. 2000;48(5):280-90.

96. Lynch P, Krasner L, Vinciquerra T, Shaffer T. Effects of intravenous perfluorocarbon and oxygen breathing on acute decompression sickness in the hamster. Undersea Biomed Res. 1989;16(4):275-81.
97. Eckmann DM, Lomivorotov VN. Microvascular gas embolization clearance following perfluorocarbon administration. J Appl Physiol (1985). 2003;94(3):860-8.
98. Leskova G, Michunskaya A, Klimenko E. Influence of perftoran on structural and metabolic disturbances in the liver during experimental atherosclerosis. Bull Exp Biol Med. 2003;136(4):340-3.
99. Maevsky E, Ivanitsky G, Bogdanova L, Axenova O, Karmen N, Zhiburt E, Senina R, Pushkin S, Maslennikov I, Orlov A. Clinical results of Perftoran application: present and future. Artif cell blood sub. 2005;33(1):37-46.
100. Dromsky DM, Spiess BD, Fahlman A. Treatment of decompression sickness in swine with intravenous perfluorocarbon emulsion. Aviat Space Environ Med. 2004;75(4):301-5.
101. Mahon RT, Watanabe TT, Wilson MC, Auker CR. Intravenous Perfluorocarbon After Onset of Decompression Sickness Decreases Mortality in 20-kg Swine. Aviat Space Environ Med. 2010;81(6):555-9.
102. Dainer H, Nelson J, Brass K, Montcalm-Smith E, Mahon R. Short oxygen prebreathing and intravenous perfluorocarbon emulsion reduces morbidity and mortality in a swine saturation model of decompression sickness. J Appl Physiol. 2007;102(3):1099-104.
103. Spahn DR, Waschke KF, Standl T, Motsch J, Van Huynegem L, Welte M, Gombotz H, Coriat P, Verkh L, Faithfull S. Use of Perflubron Emulsion to Decrease Allogeneic Blood Transfusion in High-blood-loss Non-Cardiac SurgeryResults of a European Phase 3 Study. Anesthesiology. 2002;97(6):1338-49.
104. Leese PT, Noveck RJ, Shorr JS, Woods CM, Flaim KE, Keipert PE. Randomized safety studies of intravenous perflubron emulsion. I. Effects on coagulation function in healthy volunteers. Anesth Analg. 2000;91(4):804-11.
105. Keipert PE. Oxygent™, a perfluorochemical-based oxygen therapeutic for surgical patients. In: Winslow RM, editor. Blood Substitutes: Elsevier; 2006. p. 312-23.
106. Smith CR, Parsons JT, Zhu J, Spiess BD. The effect of intravenous perfluorocarbon emulsions on whole-body oxygenation after severe decompression sickness. Diving Hyperb Med. 2012;42(1):10-7.
107. Winslow R. Current status of oxygen carriers ('blood substitutes'): 2006. Vox Sang. 2006;91(2):102-10.
108. BriceÑo JC, Rincon IE, VÉlez JF, Castro I, Arcos MI, VelÁsquez CE. Oxygen transport and consumption during experimental cardiopulmonary bypass using oxyfluor. ASAIO J. 1999;45(4):322-7.
109. Cochran RP, Kunzelman KS, Vocelka CR, Akimoto H, Thomas R, Soltow LO, Spiess BD. Perfluorocarbon emulsion in the cardiopulmonary bypass prime reduces neurologic injury. Ann Thorac Surg. 1997;63(5):1326-32.
110. Arnold J, Wagner D, Fleming J, Bird A, Grossbard E, Kaufman R, Taylor K. Cerebral protection during cardiopulmonary bypass using perfluorocarbons: a preliminary report. Perfusion. 1993;8:274.
111. Lundgren C, Bergoe G, Olszowka A, Tyssebotn I. Tissue nitrogen elimination in oxygen-breathing pigs is enhanced by fluorocarbon-derived intravascular micro-bubbles. Undersea Hyperb Med. 2005;32, No. 4, 216-26
112. Novotny J, Bridgewater B, Himm J, Homer L. Quantifying the effect of intravascular perfluorocarbon on xenon elimination from canine muscle. J Appl Physiol. 1993;74(3):1356-60.

113. Randsoe T, Hyldegaard O. Effect of oxygen breathing and perfluorocarbon emulsion treatment on air bubbles in adipose tissue during decompression sickness. J Appl Physiol. 2009;107(6):1857-63.
114. Mahon RT, Dainer HM, Nelson JW. Decompression sickness in a swine model: Isobaric denitrogenation and perfluorocarbon at depth. Aviat Space Environ Med. 2006;77(1):8-12.
115. Keipert P, Otto S, Flaim S, Weers J, Schutt E, Pelura T, Klein D, Yaksh T. Influence of perflubron emulsion particle size on blood half-life and febrile response in rats. Artif Cell Blood Sub. 1994;22(4):1169-74.
116. Riess JG. Perfluorocarbon-based oxygen delivery. Artif cell blood sub. 2006;34(6):567-80.
117. Maevsky EI, Ivanitsky HR, Islamov BI, Moroz VV, Bogdanova LA, Karmen NB, Pushkin SY, Maslennikov IA. Perftoran®. In: Winslow RM, editor. Blood Substitutes: Elsevier; 2006. p. 288-97.
118. Latson GW. 2017 Military Supplement to Shock Journal PerftoranTM (VidaphorTM) - Introduction to Western Medicine. Shock. 2017.
119. Kocian R, Spahn DR. Haemoglobin, oxygen carriers and perioperative organ perfusion. Best Pract Res Clin Anaesthesiol. 2008;22(1):63-80.
120. Keipert PE, Faithfull NS, Roth DJ, Bradley JD, Batra S, Jochelson P, Flaim KE. Supporting tissue oxygenation during acute surgical bleeding using a perfluorochemical-based oxygen carrier. In: Ince C. KJ, Telci L., Akpir K. (eds), editor. Oxygen Transport to Tissue XVII: Springer; 1996. p. 603-9.
121. Hill SE, Grocott HP, Leone BJ, White WD, Newman MF, Center NORGotDH. Cerebral physiology of cardiac surgical patients treated with the perfluorocarbon emulsion, AF0144. Ann Thorac Surg. 2005;80(4):1401-7.
122. Riess JG, Krafft MP. Fluorocarbon emulsions as in vivo oxygen delivery systems: background and chemistry. In: Winslow RM, editor. Blood substitutes: Elsevier; 2006. p. 259-75.
123. Liu S. Personal communication conversation on Oxygent on XIV ISBS Int. Symposium on Blood Substitues and Oxygen Therapeutics/ V ISNS Nanomedicine Conference Nov. 13th-15th 2017, Montreal 2017.
124. Cronin WA, Hall AA, Auker CR, Mahon RT. Perfluorocarbon in Delayed Recompression with a Mixed Gender Swine Model of Decompression Sickness. Aerosp Med Hum Perform. 2018;89(1):14-8.
125. Hall JE, Ehrhart IC, Hofman WF. Pulmonary fluid balance and hemodynamics after perfluorocarbon infusion in the dog lung. Crit Care Med. 1985;13(12):1015-9.
126. Spiess BD, Zhu JP, Pierce B, Weis R, Berger BE, Reses J, Smith CR, Ewbank B, Ward KR. Effects of Perfluorocarbon Infusion in an Anesthetized Swine Decompression Model. J Surg Res. 2009;153(1):83-94.
127. Josephson S. Pulmonary Air Embolization in the Dog: II. Evidence and Location of Pulmonary Vasoconstriction. Scand J Clin Lab. 1970;26(2):113-23.
128. Mahon RT, Cronin WA, Bodo M, Tirumala S, Regis DP, Auker CR. Cardiovascular parameters in a mixed-sex swine study of severe decompression sickness treated with the emulsified perfluorocarbon Oxycyte. J Appl Physiol. 2015;118(1):71-9.
129. Szebeni J, Baranyi L, Savay S, Bodo M, Morse DS, Basta M, Stahl GL, Bünger R, Alving CR. Liposome-induced pulmonary hypertension: properties and mechanism of a complement-mediated pseudoallergic reaction. Am J Physiol Heart Circ. 2000;279(3):H1319-H28.
130. Ellena JF, Obraztsov VV, Cumbea VL, Woods CM, Cafiso DS. Perfluorooctyl bromide has limited membrane solubility and is located at the bilayer center. Locating small molecules

in lipid bilayers through paramagnetic enhancements of NMR relaxation. J Med Chem. 2002;45(25):5534-42.
131. Rosenblum W, Hadfield M, Martinez A, Schatzki P. Alterations of liver and spleen following intravenous infusion of fluorocarbon emulsions. Arch Pathol Lab Med. 1976;100(4):213-7.
132. Fang X, Gao G, Xue H, Zhang X, Wang H. In vitro and in vivo studies of the toxic effects of perfluorononanoic acid on rat hepatocytes and Kupffer cells. Environ Toxicol Pharmacol. 2012;34(2):484-94.
133. Lutz J, Krafft M. Longitudinal studies on the interaction of perfluorochemicals with liver cytochromes P-450 by means of testing the rate of detoxification of pentobarbital. Oxygen transport to tissue XVIII: Springer; 1997. p. 391-4.
134. Obraztsov V, Shekhtman D. Effect of perfluorochemicals on liver detoxication enzymes. Artif Cell Blood Substit Immobil Biotechnol. 1994;22(4):1259-66.
135. Obraztsov V, Shekhtman D, Sklifas A, Makarov K. Analysis of the physico-chemical properties of fluorocarbon inducers of cytochrome P-450 in membranes of liver endoplasmic reticulum. Biokhimiia. 1988;53(4):613-9.
136. Lee S-J, Schlesinger PH, Wickline SA, Lanza GM, Baker NA. Simulation of fusion-mediated nanoemulsion interactions with model lipid bilayers. Soft matter. 2012;8(26):7024-35.
137. Venegas B, Wolfson MR, Cooke PH, Chong PL-G. High vapor pressure perfluorocarbons cause vesicle fusion and changes in membrane packing. Biophys J. 2008;95(10):4737-47.
138. Leal-Calderon F, Cansell M. The design of emulsions and their fate in the body following enteral and parenteral routes. Soft Matter. 2012;8(40):10213-25.
139. Wrobeln A, Schlüter KD, Linders J, Zähres M, Mayer C, Kirsch M, Ferenz KB. Functionality of albumin-derived perfluorocarbon-based artificial oxygen carriers in the Langendorff-heart. Artif Cells Nanomed Biotechnol. 2017;45(4):723-30.
140. Wrobeln A, Kirsch M, Ferenz K. Improved Albumin-Derived Perfluorocarbon-Based Artificial Oxygen Carriers: In-vivo Evaluation of Biocompatibility. Adv Biotech & Micro. 2017;7(3): 555714.
141. Du Z, Bilbao-Montoya MP, Binks BP, Dickinson E, Ettelaie R, Murray BS. Outstanding stability of particle-stabilized bubbles. Langmuir. 2003;19(8):3106-8
142. Lam S, Velikov KP, Velev OD. Pickering stabilization of foams and emulsions with particles of biological origin. Curr Opin Colloid Interface Sci. 2014;19(5):490-500.
143. Mayer D, Guerrero F, Goanvec C, Hetzel L, Linders J, Ljubkovic M, Kreczy A, Mayer C, Kirsch M, Ferenz KB. Prevention of Decompression Sickness by Novel Artificial Oxygen Carriers. Med Sci Sports Exerc. 2020.
144. Finder C, Wohlgemuth M, Mayer C. Analysis of Particle Size Distribution by Particle Tracking. Part Part Syst Charact. 2004;21(5):372-8.
145. Mazur A, Guernec A, Lautridou J, Dupas J, Dugrenot E, Belhomme M, Theron M, Guerrero F. Angiotensin Converting Enzyme Inhibitor Has a Protective Effect on Decompression Sickness in Rats. Front Physiol. 2018;9:64
146. Suzuki S, Toledo-Pereyra LH, Rodriguez FJ, Cejalvo D. Neutrophil infiltration as an important factor in liver ischemia and reperfusion injury. Modulating effects of FK506 and cyclosporine. Transplantation. 1993;55(6):1265-72.
147. Lautridou J, Buzzacott P, Belhomme M, Dugrenot E, Lafère P, Balestra C, Guerrero F. Evidence of Heritable Determinants of Decompression Sickness in Rats. Med Sci Sports Exerc. 2017;49(12):2433-8.

148. L'Abbate A, Kusmic C, Matteucci M, Pelosi G, Navari A, Pagliazzo A, Longobardi P, Bedini R. Gas embolization of the liver in a rat model of rapid decompression. Am J Physiol Regul Integr Comp Physiol. 2010;299(2):R673-R82
149. Meng W-t, Qing L, Li C-z, Zhang K, Yi H-j, Zhao X-p, Xu W-g. Ulinastatin: a potential alternative to glucocorticoid in the treatment of severe decompression sickness. Front Physiol. 2020;11:273.
150. Padnick LB, Linsenmeier RA, Goldstick TK. Perfluorocarbon emulsion improves oxygenation of the cat primary visual cortex. J Appl Physiol. 1999;86(5):1497-504.
151. Battino R, Rettich TR, Tominaga T. The solubility of nitrogen and air in liquids. J Phys Chem Ref Data. 1984;13(2):563-600.
152. Smith RM, Neuman TS. Elevation of serum creatine kinase in divers with arterial gas embolization. N Engl J Med. 1994;330(1):19-24.
153. Smith RM, Neuman TS. Abnormal serum biochemistries in association with arterial gas embolism. J Emerg Med. 1997;15(3):285-9.
154. Williams J, Collins DM, Heenan A. Creatine kinase increased after a scuba diving incident. Clin Chem. 1988;34(7):1514-5.
155. Riess JG. Reassessment of Criteria for the Selection of Perfluorochemicals for Second-Generation Blood Substitutes: Analysis of Structure/Property Relationships. Artif Organs. 1984;8(1):44-56.
156. Flaim SF. Pharmacokinetics and side effects of perfluorocarbon-based blood substitutes. Artif Cell Blood Sub. 1994;22(4):1043-54.
157. Sica A, Erreni M, Allavena P, Porta C. Macrophage polarization in pathology. Cellular and molecular life sciences. 2015;72(21):4111-26.
158. Imbert JP, Egi SM, Germonpré P, Balestra C. Static Metabolic Bubbles as precursors of vascular gas emboli during divers' decompression: a hypothesis explaining bubbling variability. Front Physiol. 2019;10:807-19
159. Mayer D, Guerrero F, Goanvec C, Hetzel L, Linders J, Ljubkovic M, Kreczy A, Mayer C, Kirsch M, Ferenz KB. Prevention of Decompression Sickness by Novel Artificial Oxygen Carriers. Med Sci Sports Exerc. 2020;52(10):2127-35.
160. Mayer D, Ferenz KB. Perfluorocarbons for the treatment of decompression illness: how to bridge the gap between theory and practice. Eur J Appl Physiol. 2019;119(11-12):2421-33.